Iranian Journal of Numerical Analysis and Optimization
Vol. 15, No. 2, 2025, pp 728–769
https://doi.org/10.22067/ijnao.2025.90299.1536
https://ijnao.um.ac.ir/

Research Article

A parameter uniform hybrid approach for singularly perturbed two-parameter parabolic problem with discontinuous data

N. Roy*, A. Jha

Abstract

In this article, we address singularly perturbed two-parameter parabolic problem of the reaction-convection-diffusion type in two dimensions. These problems exhibit discontinuities in the source term and convection coefficient at particular domain points, which result in the formation of interior layers. The presence of two perturbation parameters leads to the formation of boundary layers with varying widths. Our primary focus is to address these layers and develop a scheme that is uniformly convergent. So we propose a hybrid monotone difference scheme for the spatial direction, im-

*Corresponding author

Received 16 Actober 2024; revised 6 Febryary 2025; accepted 5 March 2025

Nirmali Roy
Department of Science and Mathematics, Indian Institute of Information Technology Guwahari, Bongora, Assam,781015. e-mail: nirmali@iiitg.ac.in

Anuradha Jha
Department of Science and Mathematics, Indian Institute of Information Technology Guwahari, Bongora, Assam,781015. e-mail: anuradha@iiitg.ac.in

How to cite this article
Roy, N. and Jha, A., A parameter uniform hybrid approach for singularly perturbed two-parameter parabolic problem with discontinuous data. *Iran. J. Numer. Anal. Optim.*, 2025; 15(2): 728-769. https://doi.org/10.22067/ijnao.2025.90299.1536

plemented on a specially designed piece-wise uniform Shishkin mesh, combined with the Crank–Nicolson method on a uniform mesh for the temporal direction. The resulting scheme is proven to be uniformly convergent, with an order of almost two in the spatial direction and exactly two in the temporal direction. Numerical experiments support the theoretically proven higher order of convergence and show that our approach results in better accuracy and convergence compared to other existing methods in the literature.

AMS subject classifications (2020): 65M06, 65M12, 65M15

Keywords: Interior layers; Hybrid Method; Singularly Perturbed; Parabolic problem; Shishkin mesh.

1 Introduction

We have considered a two-parameter singularly perturbed parabolic initial boundary value problem with nonsmooth data:

$$\begin{aligned}
&\mathcal{L}u(x,t) \equiv (\epsilon u_{xx} + \mu a u_x - bu - u_t)(x,t) = f(x,t), \qquad (x,t) \in (\Omega^- \cup \Omega^+),\\
&u(0,t) = p(t), \qquad (0,t) \in \Gamma_l = \{(0,t)|0 \le t \le T\},\\
&u(1,t) = r(t), \qquad (1,t) \in \Gamma_r = \{(1,t)|0 \le t \le T\},\\
&u(x,0) = q(x), \qquad (x,0) \in \Gamma_b = \{(x,0)|0 \le x \le 1\},
\end{aligned} \tag{1}$$

where $0 < \epsilon \ll 1$ and $0 < \mu \le 1$ are two singular perturbation parameters. Let $d \in \Gamma = (0,1)$, $\Gamma^- = (0,d)$, $\Gamma^+ = (d,1)$, $\Gamma_c = \Gamma_l \cup \Gamma_b \cup \Gamma_r$ and $\Omega = (0,1) \times (0,T]$, $\Omega^- = (0,d) \times (0,T]$, $\Omega^+ = (d,1) \times (0,T]$. The convection coefficient $a(x,t)$ and source term $f(x,t)$ experience discontinuities at $(d,t) \in \Omega$ for all t. Moreover, $a(x,t) \le -\alpha_1 < 0$ for $(x,t) \in \Omega^-$ and $a(x,t) \ge \alpha_2 > 0$ for $(x,t) \in \Omega^+$, where α_1, α_2 are positive constants. These functions are sufficiently smooth on $\Omega^- \cup \Omega^+$. We assume that the jumps of $a(x,t)$ and $f(x,t)$ at (d,t) satisfy $|[a](d,t)| < C$ and $|[f](d,t)| < C$, where the jump of ω at (d,t) is $[\omega](d,t) = \omega(d+,t) - \omega(d-,t)$. Additionally, the coefficient $b(x,t)$ is assumed to be a sufficiently smooth function on Ω such that $b(x,t) \ge \beta > 0$.

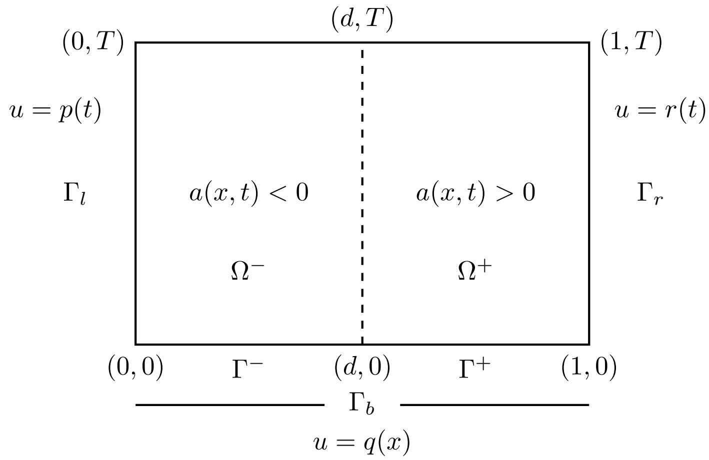

Figure 1: Domain

The boundary data $p(t), r(t)$ and initial data $q(x)$ are sufficiently smooth on the domain and satisfy the compatibility condition at the two corner points $(0,0)$ and $(1,0)$:

$$q(0) = p(0),$$

$$q(1) = r(0),$$

as well as

$$\epsilon\frac{\partial^2 q(0)}{\partial x^2} + \mu a(0)\frac{\partial q(0)}{\partial x} - b(0)q(0) - f(0,0) = \frac{\partial p(0)}{\partial t},$$

$$\epsilon\frac{\partial^2 q(1)}{\partial x^2} + \mu a(1)\frac{\partial q(1)}{\partial x} - b(1)q(1) - f(1,0) = \frac{\partial r(0)}{\partial t}.$$

Similar compatibility conditions apply at the transition point $(d,0)$; see Figure 1. Under these assumptions, the problem (1) has a unique continuous solution in the domain $\bar{\Omega}$. The solution contains strong interior layers at the points of discontinuity (d,t) for all $t \in (0,T]$ due to the discontinuity in the convection coefficient and source term. Additionally, the solution exhibits boundary layers at Γ_l and Γ_r due to the presence of perturbation parameters ϵ and μ. Singularly perturbed two-parameter parabolic problems are not extensively studied, and there is a scarcity of well-established numerical methods tailored to solve them effectively, especially in comparison to the abundance of methods available for one-parameter singularly perturbed parabolic problems. A number of researchers have developed a numerical technique for a system singularly perturbed two-parameter parabolic problems with smooth data [1, 10, 11, 14, 16, 19, 24]. Singh and Kumar [21] developed a numerical techniques for a system of singularly perturbed parabolic convection-diffusion equations. Finding a uniform numerical solution for singularly perturbed parabolic equations with discontinuous data is more challenging. For the problem (1), Chandru et al. [3, 4] showed that the accuracy of the upwind scheme on Shishkin mesh in space and the backward Euler scheme on uniform mesh in time is nearly first-order. Kumar and Kumari [12] used the Crank–Nicolson method in time on a uniform mesh and the upwind method in space on an appropriately defined Shishkin mesh to achieve a second order accurate method in time and almost first order accurate in space. Singh, Choudhary, and Kumar [22] presented an implicit scheme based on the Crank–Nicolson method in time and trigonometric B-spline basis functions on Shishkin mesh in space. This parameter uniform method is proved to be almost first order convergent in space and second order convergent in time.

With uniform meshes, standard numerical approaches cannot yield effective solution approximations in layer regions. Stynes and Roos [23] introduced a hybrid technique for steady-state singular perturbation problems (SPPs) with continuous data, which is almost of order two on a Shishkin mesh. The hybrid numerical scheme for solving singularly perturbed boundary value problems with discontinuous convection coefficients introduced by Cen [2] achieves nearly second-order accuracy across the entire domain $[0, 1]$ when the perturbation parameter ϵ satisfies $\epsilon \leq N^{-1}$. Also, Mukherjeee and Natesan [15] proposed a hybrid difference scheme on Shishkin mesh in space and Euler-backward difference in time for singularlyperturbed parabolic problems with nonsmooth data. They achieve the convergence almost two in space and first order in time.

Many problems of significance like chemical flow in reactor theory [17], fluid dynamics [20] are modeled as singularly perturbed problems. In particular, these equations are used in time-dependent semiconductor models [13]. In a drift-diffusion model, jump discontinuities in the doping profile at a p-n junction create sharp interior layers in carrier densities and electric potential. These layers significantly impact the transient behavior of semiconductor devices, such as transistor switching and charge transport.

In this paper, we have used the Crank–Nicolson scheme [5] on time on a uniform mesh and in space a hybrid scheme on piece-wise uniform Shishkin mesh. The Crank–Nicolson method in time gives second order convergence in time in supremum norm. The hybrid scheme we propose combines a modified central difference scheme, the midpoint upwind scheme, and the upwind scheme. This blending offers a key advantage: it surpasses the limitations of the classical central difference scheme. The classical central difference scheme on a uniform mesh has been found to generate nonphysical oscillations in the discrete solution when ϵ is small, unless the mesh diameter is prohibitively small. On the other hand, the midpoint upwind approach shows second-order uniform convergence beyond the boundary layer region when used with a uniform mesh. The upwind method, though first order, does not have spurious oscillations. Furthermore, the Shishkin mesh uses piece-wise uniform meshes. Thus we choose a fine mesh within the layer regions and a coarse mesh in the outer regions. Leveraging this characteristic, we utilize the second-order classical central difference scheme in the interior layer regions which is second order accurate under certain conditions. The midpoint upwind scheme and upwind scheme are used suitably in the outer region to get a monotone method. This approach allows us to accomplish nearly second-order convergence in space for the proposed hybrid scheme. Thus, the overall method has almost second order parameter uniform convergence.

Contribution in context: The main contribution of the present paper is that the numerical scheme presented here achieves order two in time and almost order two in space in the supremum norm. Also, the method is parameter uniform. The orders of convergence obtained in space in this paper is an improvement of the result of Singh, Choudhary, and Kumar [22]. The method presented there had uniform convergence of order one up to a logarithmic factor in space and order two in time in the supremum norm.

The article is arranged as follows. In Section 2, we present a *priori* bounds on the analytical solution and its derivatives. The Shishkin mesh and the detailed construction of the suggested hybrid finite difference scheme are provided in Section 3. In Section 4, the truncation error of the scheme and uniform error bound are given. In Section 5, we conduct a few numerical experiments to validate the theoretical findings and showcase the efficiency and accuracy of the proposed scheme. The primary findings are summarized in Section 6.

Notation: The norm used is the maximum norm given by

$$\|u\|_\Omega = \max_{(x,t)\in\Omega} |u(x,t)|.$$

In this study, C, C_1, or C_2 are used as a positive constants that are independent of the perturbation parameters ϵ, μ, and mesh size.

2 Analytical aspects of the solution

The analytical properties of the solution to the problem (1) are discussed in this section. The following provides details regarding the solution to (1), including the existence of a singularly perturbed solution, the minimum principle, stability bounds and a priori bounds.

Lemma 1. [12] The solution $u(x,t) \in C^0(\bar{\Omega}) \cap C^1(\Omega) \cap C^2(\Omega^- \cup \Omega^+)$ exists for (1).

Lemma 2. [12] If $u(x,t) \in C^0(\bar{\Omega}) \cap C^1(\Omega) \cap C^2(\Omega^- \cup \Omega^+)$ such that $u(x,t) \geq 0,$ for all $(x,t) \in \Gamma_c, \mathcal{L}u(x,t) \leq 0,$ for all $(x,t) \in (\Omega^- \cup \Omega^+)$ and $[u_x](d,t) \leq 0, t > 0$, then $u(x,t) \geq 0$ for all $(x,t) \in \bar{\Omega}$.

Lemma 3. [12] The bounds on $u(x,t)$ is given by

$$\|u\|_{\bar{\Omega}} \leq \|u\|_{\Gamma_c} + \frac{\|f\|_{\Omega^- \cup \Omega^+}}{\theta}.$$

where $\theta = \min\{\alpha_1/d, \alpha_2/(1-d)\}$.

The following bounds are parameter-explicit and satisfied by the derivatives of the solution to this problem (1).

Lemma 4. [3] The solution $u(x,t)$ and its derivatives for all $(x,t) \in \Omega^- \cup \Omega^+$ satisfy the following bounds for nonnegative integers k, m such that $1 \leq k + m \leq 3$:
If $\sqrt{\alpha}\mu \leq \sqrt{\rho\epsilon}$, then

$$\left\|\frac{\delta^{k+m}u}{\delta x^k\delta t^m}\right\|$$
$$\leq C\epsilon^{\frac{-k}{2}}\max\left\{\|u\|_{\bar{\Omega}},\sum_{i+2j=0}^{2}\epsilon^{i/2}\left\|\frac{\delta^{i+j}f}{\delta x^i\delta t^j}\right\|,\sum_{i=0}^{4}\left[\epsilon^{i/2}\left\|\frac{d^ip}{dt^i}\right\|_{\Gamma_l}+\left\|\frac{d^iq}{dx^i}\right\|_{\Gamma_b}+\left\|\frac{d^ir}{dt^i}\right\|_{\Gamma_r}\right]\right\}.$$

If $\sqrt{\alpha}\mu > \sqrt{\rho\epsilon}$, then

$$\left\|\frac{\delta^{k+m}u}{\delta x^k\delta t^m}\right\|$$
$$\leq C\left(\frac{\mu}{\epsilon}\right)^k\left(\frac{\mu^2}{\epsilon}\right)^m\max\left\{\|u\|_{\bar{\Omega}},\sum_{i+2j=0}^{2}\left(\frac{\epsilon}{\mu}\right)^i\left(\frac{\epsilon}{\mu^2}\right)^{j+1}\left\|\frac{\delta^{i+j}f}{\delta x^i\delta t^j}\right\|,\right.$$
$$\left.\sum_{i=0}^{4}\left[\left(\frac{\epsilon}{\mu}\right)^i\left\|\frac{d^ip}{dt^i}\right\|_{\Gamma_l}+\left(\frac{\epsilon}{\mu^2}\right)^{j+1}\left\|\frac{d^iq}{dx^i}\right\|_{\Gamma_b}+\left(\frac{\epsilon}{\mu^2}\right)^{j+1}\left\|\frac{d^ir}{dt^i}\right\|_{\Gamma_r}\right]\right\},$$

where C is a constant independent of ϵ and μ.

To obtain sharper bounds on the solution, the solution $u(x,t)$ of (1) is decomposed into regular and layers components as $u(x,t) = v(x,t)+w_l(x,t)+w_r(x,t)$. The regular component $v(x,t)$ satisfies the following equation:

$$\begin{aligned}&\mathcal{L}v(x,t) = f(x,t), && (x,t)\in\Omega^-\cup\Omega^+,\\ &v(x,0) = u(x,0), && \text{for all } x\in\Gamma^-\cup\Gamma^+,\end{aligned} \tag{2}$$

and $v(0,t), v(1,t), v(d-,t), v(d+,t)$ are chosen suitably for all t in $(0,T]$. Also, $v(d-,t) = \lim_{x\to d^-} v(x,t)$ and $v(d+,t) = \lim_{x\to d^+} v(x,t)$. The regular component $v(x,t)$ can further be decomposed as

$$v(x,t) = \begin{cases} v^-(x,t), & (x,t)\in\Omega^-,\\ v^+(x,t), & (x,t)\in\Omega^+,\end{cases}$$

where $v^-(x,t)$ and $v^+(x,t)$ are the left and right regular components, respectively.

The singular components $w_l(x,t)$ and $w_r(x,t)$ are the solutions of

$$\begin{aligned}&\mathcal{L}w_l(x,t) = 0, && (x,t)\in\Omega^-\cup\Omega^+,\\ &w_l(0,t) = u(0,t)-v(0,t)-w_r(0,t), && \text{for all } t\in(0,T],\\ &w_l(1,t) \text{ is chosen suitably} && \text{for all } t\in(0,T],\\ &w_l(x,0) = 0, && \text{for all } x\in\Gamma^-\cup\Gamma^+,\end{aligned} \tag{3}$$

and

$$
\begin{aligned}
&\mathcal{L}w_r(x,t)=0, \qquad (x,t)\in\Omega^-\cup\Omega^+,\\
&w_r(0,t) \text{ is chosen suitably} \qquad \text{for all } t\in(0,T],\\
&w_r(1,t)=u(1,t)-v(1,t)-w_l(1,t), \qquad \text{for all } t\in(0,T],\\
&w_r(x,0)=0, \qquad \text{for all } x\in\Gamma^-\cup\Gamma^+,
\end{aligned}
\tag{4}
$$

respectively. The regular v and layer w_l, w_r components may be discontinuous at (d,t), for all $t\in(0,T]$ but their sum u is continuous at (d,t), for all $t\in(0,T]$. Furthermore, the singular components $w_l(x,t)$ and $w_r(x,t)$ are decomposed as

$$
w_l(x,t)=\begin{cases} w_l^-(x,t), & (x,t)\in\Omega^-,\\ w_l^+(x,t), & (x,t)\in\Omega^+,\end{cases}\quad w_r(x,t)=\begin{cases} w_r^-(x,t), & (x,t)\in\Omega^-,\\ w_r^+(x,t), & (x,t)\in\Omega^+.\end{cases}
$$

Hence, the unique solution $u(x,t)$ to (1) is written as

$$
u(x,t)=\begin{cases}
(v^-+w_l^-+w_r^-)(x,t), & (x,t)\in\Omega^-,\\
(v^-+w_l^-+w_r^-)(d-,t) & \\
=(v^++w_l^++w_r^+)(d+,t), & (x,t)=(d,t),\ \text{for all } \ t\in(0,T],\\
(v^++w_l^++w_r^+)(x,t), & (x,t)\in\Omega^+.
\end{cases}
$$

Lemma 5. The bounds on the components $v(x,t), w_l(x,t), w_r(x,t)$ and their derivatives are given as follows for $\sqrt{\alpha}\mu\le\sqrt{\rho\epsilon}$ and $0\le i+2j\le 4$:

$$
\left\|\frac{\delta^{i+j}v}{\delta x^i\delta t^j}\right\|_{\Omega^-\cup\Omega^+}\le C(1+\epsilon^{(3-i)/2}),
$$

$$
\left\|\frac{\delta^{i+j}w_l}{\delta x^i\delta t^j}\right\|_{\Omega^-\cup\Omega^+}\le C\epsilon^{-i/2}\begin{cases} e^{-\theta_2 x}, & (x,t)\in\Omega^-,\\ e^{-\theta_1(x-d)}, & (x,t)\in\Omega^+,\end{cases}
$$

$$
\left\|\frac{\delta^{i+j}w_r}{\delta x^i\delta t^j}\right\|_{\Omega^-\cup\Omega^+}\le C\epsilon^{-i/2}\begin{cases} e^{-\theta_1(d-x)}, & (x,t)\in\Omega^-,\\ e^{-\theta_2(1-x)}, & (x,t)\in\Omega^+,\end{cases}
$$

where

$$
\theta_1=\frac{\sqrt{\rho\alpha}}{\sqrt{\epsilon}},\qquad \theta_2=\frac{\sqrt{\rho\alpha}}{2\sqrt{\epsilon}}, \tag{5}
$$

and C is a constant independent of ϵ and μ.

Proof. The proof follows by following the approach given in Gracia and O'Riordan [9]. □

Lemma 6. The bounds on the components $v(x,t), w_l(x,t), w_r(x,t)$ and their derivatives are given as follows for $\sqrt{\alpha}\mu > \sqrt{\rho\epsilon}$ and $0 \le i+2j \le 4$,:

$$\left\| \frac{\delta^{i+j} v}{\delta x^i \delta t^j} \right\|_{\Omega^- \cup \Omega^+} \le C(1 + (\epsilon/\mu)^{(3-i)}),$$

$$\left\| \frac{\delta^{i+j} w_l}{\delta x^i \delta t^j} \right\|_{\Omega^- \cup \Omega^+} \le C\left(\frac{\mu}{\epsilon}\right)^i \begin{cases} e^{-\theta_2 x}, & (x,t) \in \Omega^-, \\ e^{-\theta_1(x-d)}, & (x,t) \in \Omega^+, \end{cases}$$

$$\left\| \frac{\delta^{i+j} w_r}{\delta x^i \delta t^j} \right\|_{\Omega^- \cup \Omega^+} \le C\left(\frac{1}{\mu}\right)^i \begin{cases} e^{-\theta_1(d-x)}, & (x,t) \in \Omega^-, \\ e^{-\theta_2(1-x)}, & (x,t) \in \Omega^+, \end{cases}$$

where

$$\theta_1 = \frac{\alpha\mu}{\epsilon}, \qquad \theta_2 = \frac{\rho}{2\mu}, \tag{6}$$

and C is a constant independent of ϵ and μ.

Proof. For the proof, refer to the idea given in Gracia and O'Riordan [9]. □

3 Discretization

We will first discretize (1) in time using the Crank–Nicolson method [5]. This results in a semidiscrete system of equations. We then discretize in space.

3.1 Discretization in time

We begin by demonstrating the semidiscretization of the problem in the temporal direction on a uniform mesh using the Crank–Nicolson method [5]. For a fixed time T, the interval $[0,T]$ is partitioned uniformly as $\Lambda^M = \{t_j = j\Delta t : j = 0,1,\dots,M, \Delta t = \frac{T}{M}\}$. The semidiscretization yields the following system of linear ordinary differential equations:

$$\begin{aligned} &\epsilon U_{xx}^{j+\frac{1}{2}}(x) + \mu a^{j+\frac{1}{2}}(x) U_x^{j+\frac{1}{2}}(x) - b^{j+\frac{1}{2}}(x) U^{j+\frac{1}{2}}(x) \\ &= f^{j+\frac{1}{2}}(x) + \frac{U^{j+1}(x) - U^j(x)}{\Delta t}, \end{aligned}$$

$$
\begin{aligned}
&\qquad\qquad\qquad\qquad\qquad\qquad x \in (\Omega^- \cup \Omega^+),\ 0 \le j \le M-1,\\
&U^{j+1}(0) = u(0, t_{j+1}), \qquad U^{j+1}(1) = u(1, t_{j+1}), \quad 0 \le j \le M-1,\\
&U^0(x) = u(x, 0), \qquad x \in \Gamma_b,
\end{aligned}
$$

where $U^{j+1}(x)$ is the approximation of $u(x, t_{j+1})$ of (1) at $(j+1)$th time level and $p^{j+\frac{1}{2}} = \dfrac{p^{j+1}(x) + p^j(x)}{2}$. Upon simplification, we have

$$
\left.
\begin{aligned}
&\widetilde{\mathcal{L}}U^{j+1}(x) = g(x, t_{j+1}),\ \ x \in (\Gamma^- \cup \Gamma^+), \qquad 0 \le j \le M-1,\\
&U^{j+1}(0) = u(0, t_{j+1}), \quad 0 \le j \le M-1,\\
&U^{j+1}(1) = u(1, t_{j+1}), \quad 0 \le j \le M-1,\\
&U^0(x) = u(x, 0), \qquad\quad x \in \Gamma,
\end{aligned}
\right\}
\tag{7}
$$

where the operator $\widetilde{\mathcal{L}}$ is defined as

$$
\widetilde{\mathcal{L}} \equiv \epsilon \frac{d^2}{dx^2} + \mu a^{j+\frac{1}{2}} \frac{d}{dx} - c^{j+\frac{1}{2}} I,
$$

and

$$
\begin{aligned}
g(x, t_{j+1}) &= 2f^{j+\frac{1}{2}}(x) - \epsilon U^j_{xx}(x) - \mu a^{j+\frac{1}{2}}(x) U^j_x(x) + d^{j+\frac{1}{2}}(x) U^j(x),\\
c^{j+\frac{1}{2}}(x) &= b^{j+\frac{1}{2}}(x) + \frac{2}{\Delta t},\\
d^{j+\frac{1}{2}}(x) &= b^{j+\frac{1}{2}}(x) - \frac{2}{\Delta t}.
\end{aligned}
$$

The error in temporal semidiscretization is defined by $e^{j+1} = u(x, t_{j+1}) - \hat{U}^{j+1}(x)$, where $u(x, t_{j+1})$ is the solution of (1). Moreover, $\hat{U}^{j+1}(x)$ is the solution of semidiscrete scheme (7), when $u(x, t_j)$ is taken instead of U^j to find solution at (x, t_{j+1}).

Theorem 1. The local truncation error $T_{j+1} = \widetilde{\mathcal{L}}(e^{j+1})$ satisfies

$$
\|T_{j+1}\| \le C(\Delta t)^3, \qquad 0 \le j \le M-1.
$$

Proof. The Taylor's approximation gives

$$
\begin{aligned}
u(x, t_{j+1}) &= u(x, t_{j+\frac{1}{2}}) + \frac{1}{2}\Delta t u_t(x, t_{j+\frac{1}{2}}) + \frac{1}{8}\Delta t^2 u_{tt}(x, t_{j+\frac{1}{2}}) + \mathcal{O}(\Delta t)^3,\\
u(x, t_j) &= u(x, t_{j+\frac{1}{2}}) - \frac{1}{2}\Delta t u_t(x, t_{j+\frac{1}{2}}) + \frac{1}{8}\Delta t^2 u_{tt}(x, t_{j+\frac{1}{2}}) + \mathcal{O}(\Delta t)^3.
\end{aligned}
$$

Using these equations, we have

$$\begin{aligned}\frac{u(x,t_{j+1})-u(x,t_j)}{\Delta t} =& u_t(x,t_{j+\frac{1}{2}})+\mathcal{O}(\Delta t)^2\\ =&\epsilon u_{xx}(x,t_{j+\frac{1}{2}})+\mu a(x,t_{j+\frac{1}{2}})u_x(x,t_{j+\frac{1}{2}})\\ &-b(x,t_{j+\frac{1}{2}})u(x,t_{j+\frac{1}{2}})-f(x,t_{j+\frac{1}{2}})+\mathcal{O}(\Delta t)^2.\end{aligned}$$

Further simplification gives

$$\begin{aligned}\widetilde{\mathcal{L}}u_x^j &= \epsilon u_{xx}(x,t_{j+1})+\mu a^{j+\frac{1}{2}}u_x(x,t_{j+1})-c^{j+\frac{1}{2}}u(x,t_{j+1})\\ &= g(x,t_{j+1})+\mathcal{O}(\Delta t)^3.\end{aligned}$$

Hence the local truncation error satisfies

$$\begin{aligned}&\widetilde{\mathcal{L}}(e^{j+1})=\mathcal{O}(\Delta t)^3,\\ &e^{j+1}(0)=e^{j+1}(0)=0.\end{aligned}$$

We arrive at the result using Lemma 3. [14]) $e^{j+1}(x)\leq \mathcal{O}(\Delta t)^3$. □

Theorem 2. The global error $E^j=u(x,t_j)-U^j(x)$ is estimated as

$$\|E^j\|\leq C(\Delta t)^2, \qquad 0\leq j\leq M-1,$$

where $U^j(x)$ is the solution of (7).

Proof. For proof, refer to [22]. $\|\prod_{k=0}^{i-1}R_{j-k}\|\leq C, \quad$ for all $i=1,2,3,...j, 1\leq j\leq M$. □

3.2 Discretization in space

We understand from the relevant literature on SPPs that a uniform mesh is insufficient for achieving uniform convergence of (1) due to the existence of layer regions. The differential equation (1) exhibits strong interior layers including boundary layers near the boundaries. To resolve these layers, we have discretized this problem by using a piece-wise uniform Shishkin mesh.

Let the interior points of the spatial mesh be denoted by $\Gamma^N=\{x_i: 1\leq i\leq \frac{N}{2}-1\}\cup\{x_i:\frac{N}{2}+1\leq i\leq N-1\}$. The equation $\bar{\Gamma}^N=\{x_i\}_0^N\cup\{d\}$ denotes the mesh points with $x_0 = 0, x_N = 1$ and the point of discontinuity at point $x_{\frac{N}{2}} = d$. We also introduce the notation $\Gamma^{N-} = \{x_i\}_0^{\frac{N}{2}-1}, \Gamma^{N+} = \{x_i\}_{\frac{N}{2}+1}^{N-1}$, $\Omega^{N-} = \Gamma^{N-} \times \Lambda^M$, $\Omega^{N+} = \Gamma^{N+} \times \Lambda^M$, $\Omega^{N,M} = \Gamma^N \times \Lambda^M, \bar{\Omega}^{N,M} = \bar{\Gamma}^N \times \Lambda^M$, $\Gamma_c^N = \bar{\Omega}^{N,M} \cap \Gamma_c$, $\Gamma_l^N = \Gamma_c^N \cap \Gamma_l$, $\Gamma_b^N = \Gamma_c^N \cap \Gamma_b$ and $\Gamma_r^N = \Gamma_c^N \cap \Gamma_r$. The domain $[0, 1]$ is subdivided into six subintervals as

$$\bar{\Gamma} = [0, \tau_1] \cup [\tau_1, d - \tau_2] \cup [d - \tau_2, d] \cup [d, d + \tau_3] \cup [d + \tau_3, 1 - \tau_4] \cup [1 - \tau_4, 1] = \bigcup_{i=1}^{6} I_i.$$

The transition points in $\bar{\Gamma}$ are

$$\tau_1 = \min\left\{\frac{d}{4}, \frac{2}{\theta_2}\ln N\right\}, \qquad \tau_2 = \min\left\{\frac{d}{4}, \frac{2}{\theta_1}\ln N\right\},$$

$$\tau_3 = \min\left\{\frac{1-d}{4}, \frac{2}{\theta_1}\ln N\right\}, \qquad \tau_4 = \min\left\{\frac{1-d}{4}, \frac{2}{\theta_2}\ln N\right\}.$$

On the subintervals $[0, \tau_1], [d - \tau_2, d], [d, d + \tau_3]$, and $[1 - \tau_4, 1]$, a uniform mesh of $\left(\frac{N}{8} + 1\right)$ mesh points and on $[\tau_1, d - \tau_2]$ and $[d + \tau_3, 1 - \tau_4]$ a uniform mesh of $\left(\frac{N}{4} + 1\right)$ mesh points are taken. The mesh points are given by

$$x_i = \begin{cases} \dfrac{8i\tau_1}{N}, & 0 \le i \le \frac{N}{8}, \\ \tau_1 + \dfrac{4(d - \tau_1 - \tau_2)}{N}\left(i - \dfrac{N}{8}\right), & \frac{N}{8} \le i \le \frac{3N}{8}, \\ d - \tau_2 + \dfrac{8\tau_2}{N}\left(i - \dfrac{3N}{8}\right), & \frac{3N}{8} \le i \le \frac{N}{2}, \\ d + \dfrac{8\tau_3}{N}\left(i - \dfrac{N}{2}\right), & \frac{N}{2} \le i \le \frac{5N}{8}, \\ d + \tau_3 + \dfrac{4(1 - d - \tau_3 - \tau_4)}{N}\left(i - \dfrac{5N}{8}\right), & \frac{5N}{8} \le i \le \frac{7N}{8}, \\ 1 - \tau_4 + \dfrac{8\tau_4}{N}\left(i - \dfrac{7N}{8}\right), & \frac{7N}{8} \le i \le N. \end{cases}$$

Let $h_i = x_i - x_{i-1}$ denote the step size and let $h_1 = \frac{8\tau_1}{N}, h_2 = \frac{4(d-\tau_1-\tau_2)}{N}, h_3 = \frac{8\tau_2}{N}, h_4 = \frac{8\tau_3}{N}, h_5 = \frac{4(1-d-\tau_3-\tau_4)}{N}, h_6 = \frac{8\tau_4}{N}$ denote the step sizes in the interval I_1, I_2, I_3, I_4, I_5, and I_6, respectively.

Assumption 1. Throughout the paper, we shall also assume that $\epsilon \le N^{-1}$ as is generally the case for discretization of convection-dominated problems.

We have presented a hybrid difference approach for the discretization of the problem (1) in the spatial variable. On the above piece-wise uniform Shishkin mesh, this hybrid difference scheme comprises of an upwind, a central difference and a midpoint upwind scheme. Here, we introduce the hybrid difference method for the ratio $\sqrt{\alpha}\mu \leq \sqrt{\rho\epsilon}$:

$$\mathcal{L}_h^{N,M}U^{j+1}(x_i) = \begin{cases} \mathcal{L}_c^{N,M}U^{j+1}(x_i), & x_i \in (0,1)\backslash\{\tau_1, d-\tau_2, d, d+\tau_3, 1-\tau_4\}, \\ & \text{with } \mu\|a\|h_k < 2\epsilon,\ 1 \leq k \leq 6, \\ \mathcal{L}_t^{N,M}U^{j+1}(x_{\frac{N}{2}}), & x_i = d \text{ with } h_k(\|b\| + \frac{2}{\Delta t}) < 2\mu\alpha,\ k = 3,4. \end{cases}$$

For the ratio $\sqrt{\alpha}\mu > \sqrt{\rho\epsilon}$, we use

$$\mathcal{L}_h^{N,M}U^{j+1}(x_i) = \begin{cases} \mathcal{L}_m^{N,M}U^{j+1}(x_i), & x_i \in (0,\tau_1) \cup (\tau_1, d-\tau_2), \\ & \text{with } (\|b\| + \frac{2}{\Delta t})h_k \leq 2\alpha\mu,\ k = 1,2, \\ \mathcal{L}_u^{N,M}U^{j+1}(x_i), & x_i \in (0,\tau_1) \cup (\tau_1, d-\tau_2), \\ & \text{with } (\|b\| + \frac{2}{\Delta t})h_k > 2\alpha\mu,\ k = 1,2, \\ \mathcal{L}_c^{N,M}U^{j+1}(x_i), & x_i \in (d-\tau_2, d) \cup (d, d+\tau_3), \\ & \text{with } \mu\|a\|h_k < 2\epsilon,\ k = 3,4, \\ \mathcal{L}_m^{N,M}U^{j+1}(x_i), & x_i \in (d+\tau_3, 1-\tau_4) \cup (1-\tau_4, 1), \\ & \text{with } (\|b\| + \frac{2}{\Delta t})h_k \leq 2\alpha\mu,\ k = 5,6, \\ \mathcal{L}_u^{N,M}U^{j+1}(x_i), & x_i \in (d+\tau_3, 1-\tau_4) \cup (1-\tau_4, 1), \\ & \text{with } (\|b\| + \frac{2}{\Delta t})h_k > 2\alpha\mu,\ k = 5,6, \\ \mathcal{L}_t^{N,M}U^{j+1}(x_{\frac{N}{2}}), & x_i = d \text{ with } h_k(\|b\| + \frac{2}{\Delta t}) < 2\mu\alpha,\ k = 3,4. \end{cases}$$

At the transition points for both case

$$\mathcal{L}_h^{N,M}U^{j+1}(x_i) = \begin{cases} \mathcal{L}_m^{N,M}U^{j+1}(x_i),\ (\|b\| + \frac{2}{\Delta t})h_k \leq 2\alpha\mu, & k = 2,3,5,6, \\ \mathcal{L}_u^{N,M}U^{j+1}(x_i), \quad \text{otherwise}. \end{cases}$$

The fully discretize scheme is given by

$$\mathcal{L}_h^{N,M}U^{j+1}(x_i) \equiv r_i^- U^{j+1}(x_{i-1}) + r_i^c U^{j+1}(x_i) + r_i^+ U^{j+1}(x_{i+1}) = g^{j+1}(x_i). \tag{8}$$

At the point of discontinuity $x_{N/2} = d$, we have used five point second order difference scheme

$$\mathcal{L}_t^{N,M} U^{j+1}(x_{\frac{N}{2}}) = \frac{-U^{j+1}(x_{N/2+2}) + 4U^{j+1}(x_{\frac{N}{2}+1}) - 3U^{j+1}(x_{\frac{N}{2}})}{2h_4} - \frac{U^{j+1}(x_{\frac{N}{2}-2}) - 4U^{j+1}(x_{\frac{N}{2}-1}) + 3U^{j+1}(x_{\frac{N}{2}})}{2h_3} = 0. \tag{9}$$

Associated with each of these finite difference operators, we have the following finite difference scheme:

$$\mathcal{L}_c^{N,M} U^{j+1}(x_i) \equiv \epsilon\delta^2 U^{j+1}(x_i) + \mu a^{j+\frac{1}{2}}(x_i) D^0 U^{j+1}(x_i) - b^{j+\frac{1}{2}}(x_i) U^{j+1}(x_i),$$
$$\mathcal{L}_m^{N,M} U^{j+1}(x_i) \equiv \epsilon\delta^2 U^{j+1}(x_i) + \mu \bar{a}^{j+\frac{1}{2}}(x_i) D^* U^{j+1}(x_i) - \bar{b}^{j+\frac{1}{2}}(x_i) \bar{U}^{j+1}(x_i),$$
$$\mathcal{L}_u^{N,M} U^{j+1}(x_i) \equiv \epsilon\delta^2 U^{j+1}(x_i) + \mu a^{j+\frac{1}{2}}(x_i) D^* U^{j+1}(x_i) - b^{j+\frac{1}{2}}(x_i) U^{j+1}(x_i),$$

and

$$g^{j+1}(x_i) = \begin{cases} 2f^{j+\frac{1}{2}}(x_i) - \epsilon\delta_x^2 U^j(x_i) - \mu a^{j+\frac{1}{2}}(x_i) D_x^0 U^j(x_i) + d^{j+\frac{1}{2}}(x) U^j(x_i), & \mathcal{L}_h^{N,M} = \mathcal{L}_c^{N,M}, \\ 2f^{j+\frac{1}{2}}(x_i) - \epsilon\delta_x^2 U^j(x_i) - \mu \bar{a}^{j+\frac{1}{2}}(x_i) D_x^* U^j(x_i) + \bar{d}^{j+\frac{1}{2}}(x) U^j(x_i), & \mathcal{L}_h^{N,M} = \mathcal{L}_m^{N,M}, \\ 2f^{j+\frac{1}{2}}(x_i) - \epsilon\delta_x^2 U^j(x_i) - \mu a^{j+\frac{1}{2}}(x_i) D_x^* U^j(x_i) + d^{j+\frac{1}{2}}(x) U^j(x_i), & \mathcal{L}_h^{N,M} = \mathcal{L}_u^{N,M}, \end{cases}$$

where

$$D^+ U^{j+1}(x_i) = \frac{U^{j+1}(x_{i+1}) - U^{j+1}(x_i)}{x_{i+1} - x_i}, \qquad D^- U^{j+1}(x_i) = \frac{U^{j+1}(x_i) - U^{j+1}(x_{i-1})}{x_i - x_{i-1}},$$

$$D^0 U^{j+1}(x_i) = \frac{U^{j+1}(x_{i+1}) - U^{j+1}(x_{i-1})}{h_{i+1} + h_i},$$

$$\delta^2 U^{j+1}(x_i) = \frac{2(D^+ U^{j+1}(x_i) - D^- U^{j+1}(x_i))}{x_{i+1} - x_{i-1}},$$

$$D^* U^{j+1}(x_i) = \begin{cases} D^- U^{j+1}(x_i), \ i < \frac{N}{2}, \\ D^+ U^{j+1}(x_i), \ i > \frac{N}{2}, \end{cases}$$

$\hbar_i = \frac{h_i + h_{i+1}}{2}$, $\quad \bar{w}^{j+1}(x_i) = \dfrac{w^{j+1}(x_i) + w^{j+1}(x_{i-1})}{2}$ in Ω^{N-},

$\bar{w}^{j+1}(x_i) = \dfrac{w^{j+1}(x_i) + w^{j+1}(x_{i+1})}{2}$ in Ω^{N+}, $\bar{a}^{j+\frac{1}{2}}(x_i) = \dfrac{\bar{a}^{j+1}(x_i) + \bar{a}^j(x_i)}{2}$,

$\bar{b}^{j+\frac{1}{2}}(x_i) = \dfrac{\bar{b}^{j+1}(x_i) + \bar{b}^j(x_i)}{2}$ and $\bar{d}^{j+\frac{1}{2}}(x_i) = \dfrac{\bar{d}^{j+1}(x_i) + \bar{d}^j(x_i)}{2}$.

The matrix associated with the above equations (8) is not an M-matrix. We transform (9) to establish the monotonicity property by estimating $U^{j+1}_{\frac{N}{2}-2}$ and $U^{j+1}_{\frac{N}{2}+2}$ for $\mathcal{L}_t^{N,M}U^{j+1}(x_i)$.

For $\sqrt{\alpha}\mu \le \sqrt{\rho}\epsilon$ and $\sqrt{\alpha}\mu > \sqrt{\rho}\epsilon$, from the operator $\mathcal{L}_c^{N,M}$, we get

$$\begin{aligned}
&U^{j+1}_{N/2-2}\\
&= \frac{2h_3^2}{2\epsilon - \mu h_3 a^{j+\frac{1}{2}}_{N/2-1}}\Bigg\{g^{j+1}_{N/2-1} - U^{j+1}_{N/2-1}\left(\frac{-2\epsilon - h_3^2(b^{j+\frac{1}{2}}_{N/2-1} + \frac{2}{\Delta t})}{h_3^2}\right)\\
&\qquad - U^{j+1}_{N/2}\left(\frac{2\epsilon + \mu h_3 a^{j+\frac{1}{2}}_{N/2-1}}{2h_3^2}\right)\Bigg\}\\
&U^{j+1}_{N/2+2}\\
&= \frac{2h_4^2}{2\epsilon + \mu h_4 a^{j+\frac{1}{2}}_{N/2+1}}\Bigg\{g^{j+1}_{N/2+1} - U^{j+1}_{N/2+1}\left(\frac{-2\epsilon - h_4^2(b^{j+\frac{1}{2}}_{N/2+1} + \frac{2}{\Delta t})}{h_4^2}\right)\\
&\qquad - U^{j+1}_{N/2}\left(\frac{2\epsilon - \mu h_4 a^{j+\frac{1}{2}}_{N/2+1}}{2h_4^2}\right)\Bigg\}.
\end{aligned}$$

Inserting the above expression in $\mathcal{L}_t^{N,M}U^{j+1}(x_{N/2})$, we get a tridiagonal system of equations of the following form:

$$\begin{aligned}
\mathcal{L}_t^{N,M}U^{j+1}_{N/2} =& \left(\frac{2\epsilon - h_4\mu a^{j+\frac{1}{2}}_{N/2+1}}{2\epsilon + h_4\mu a^{j+\frac{1}{2}}_{N/2+1}}h_3 - 3(h_3+h_4) + \frac{2\epsilon + h_3\mu a^{j+\frac{1}{2}}_{N/2-1}}{2\epsilon - h_3\mu a^{j+\frac{1}{2}}_{N/2-1}}h_4\right)U^{j+1}_{N/2}\\
&+ \left(\frac{-4\epsilon - 2h_4^2(b^{j+\frac{1}{2}}_{N/2+1} + \frac{2}{\Delta t})}{2\epsilon + h_4\mu a^{j+\frac{1}{2}}_{N/2+1}} + 4\right)h_3 U^{j+1}_{N/2+1}\\
&+ \left(\frac{-4\epsilon - 2h_3^2(b^{j+\frac{1}{2}}_{N/2-1} + \frac{2}{\Delta t})}{2\epsilon - h_3\mu a^{j+\frac{1}{2}}_{N/2-1}} + 4\right)h_4 U^{j+1}_{N/2-1}\\
=& \frac{2h_3^2 h_4 g^{j+1}_{N/2-1}}{2\epsilon - h_3\mu a^{j+\frac{1}{2}}_{N/2-1}} + \frac{2h_4^2 h_3 g^{j+1}_{N/2+1}}{2\epsilon + h_4\mu a^{j+\frac{1}{2}}_{N/2+1}}.
\end{aligned}$$

The element of the system matrix $\mathcal{L}_h^{N,M}$ is as follows:
In $\Omega^- \cup \Omega^+$, if $\mathcal{L}_h^{N,M} = \mathcal{L}_c^{N,M}$, then

$$r_i^- = \frac{\epsilon}{h_i \hbar_i} - \frac{\mu a^{j+\frac{1}{2}}(x_i)}{2\hbar_i}, \qquad r_i^+ = \frac{\epsilon}{h_{i+1}\hbar_i} + \frac{\mu a^{j+\frac{1}{2}}(x_i)}{2\hbar_i},$$

$$r_i^c = -r_i^- - r_i^+ - \left(b^{j+\frac{1}{2}}(x_i) + \frac{2}{\Delta t}\right).$$

In Ω^-, if $\mathcal{L}_h^{N,M} = \mathcal{L}_m^{N,M}$, then

$$r_i^- = \frac{\epsilon}{h_i \hbar_i} - \frac{\mu \bar{a}^{j+\frac{1}{2}}(x_i)}{h_i} - \left(\frac{\bar{b}^{j+\frac{1}{2}}(x_i)}{2} + \frac{1}{\Delta t}\right), \qquad r_i^+ = \frac{\epsilon}{h_{i+1}\hbar_i},$$

$$r_i^c = -r_i^- - r_i^+ - \frac{1}{2}\left(\bar{b}^{j+\frac{1}{2}}(x_i) + \frac{2}{\Delta t}\right).$$

In Ω^+, if $\mathcal{L}_h^{N,M} = \mathcal{L}_m^{N,M}$, then

$$r_i^- = \frac{\epsilon}{h_i \hbar_i}, \qquad r_i^+ = \frac{\epsilon}{h_{i+1}\hbar_i} - \frac{\mu \bar{a}^{j+\frac{1}{2}}(x_i)}{h_{i+1}} - \left(\frac{\bar{b}^{j+\frac{1}{2}}(x_i)}{2} + \frac{1}{\Delta t}\right),$$

$$r_i^c = -r_i^- - r_i^+ - \frac{1}{2}\left(\bar{b}^{j+\frac{1}{2}}(x_i) + \frac{2}{\Delta t}\right).$$

In Ω^-, if $\mathcal{L}_h^{N,M} = \mathcal{L}_u^{N,M}$, then

$$r_i^- = \frac{\epsilon}{h_i \hbar_i} - \frac{\mu a^{j+\frac{1}{2}}(x_i)}{h_i}, \qquad r_i^+ = \frac{\epsilon}{h_{i+1}\hbar_i},$$

$$r_i^c = -r_i^- - r_i^+ - \left(b^{j+\frac{1}{2}}(x_i) + \frac{2}{\Delta t}\right).$$

In Ω^+, if $\mathcal{L}_h^{N,M} = \mathcal{L}_u^{N,M}$, then

$$r_i^- = \frac{\epsilon}{h_i \hbar_i}, \qquad r_i^+ = \frac{\epsilon}{h_{i+1}\hbar_i} + \frac{\mu a^{j+\frac{1}{2}}(x_i)}{h_{i+1}},$$

$$r_i^c = -r_i^- - r_i^+ - \left(b^{j+\frac{1}{2}}(x_i) + \frac{2}{\Delta t}\right).$$

At $x_{N/2} = d$,

we have

$$r_{N/2}^- = \left(\frac{-4\epsilon - 2h_3^2(b_{N/2-1}^{j+\frac{1}{2}} + \frac{2}{\Delta t})}{2\epsilon - h_3 \mu a_{N/2-1}^{j+\frac{1}{2}}} + 4\right) h_4,$$

$$r_{N/2}^+ = \left(\frac{-4\epsilon - 2h_4^2(b_{N/2+1}^{j+\frac{1}{2}} + \frac{2}{\Delta t})}{2\epsilon + h_4 \mu a_{N/2+1}^{j+\frac{1}{2}}} + 4\right) h_3,$$

$$r^c_{N/2} = \Bigg(\frac{2\epsilon - h_4\mu a^{j+\frac{1}{2}}_{N/2+1}}{2\epsilon + h_4\mu a^{j+\frac{1}{2}}_{N/2+1}} h_3 - 3(h_3+h_4) + \frac{2\epsilon + h_3\mu a^{j+\frac{1}{2}}_{N/2-1}}{2\epsilon - h_3\mu a^{j+\frac{1}{2}}_{N/2-1}} h_4\Bigg).$$

To guarantee that the operator $\mathcal{L}_h^{N,M}$ is monotone, we impose the following assumption:

$$N(\ln N)^{-1} > 16 \max\left\{\frac{\|b\|}{\alpha}, \frac{(\|b\| + \frac{2}{\Delta t})}{\alpha\rho}\right\}. \tag{10}$$

To find the error estimates for the scheme (8) defined above, we first decompose the discrete solution $U(x_i, t_{j+1})$ into the discrete regular and discrete singular components.

Let

$$U^{j+1}(x_i) = V^{j+1}(x_i) + W_l^{j+1}(x_i) + W_r^{j+1}(x_i).$$

The discrete regular components is

$$V^{j+1}(x_i) = \begin{cases} V^{-(j+1)}(x_i), & (x_i, t_{j+1}) \in \Omega^{N-}, \\ V^{+(j+1)}(x_i), & (x_i, t_{j+1}) \in \Omega^{N+}, \end{cases}$$

where $V^{-(j+1)}(x_i)$ and $V^{+(j+1)}(x_i)$ approximate $v^-(x_i, t_{j+1})$ and $v^+(x_i, t_{j+1})$, respectively. They satisfy the following equations:

$$\left.\begin{array}{ll} \mathcal{L}_h^{N,M} V^{-(j+1)}(x_i) = g(x_i, t_{j+1}), & \text{for all } (x_i, t_{j+1}) \in \Omega^{N-}, \\ V^{-(j+1)}(x_0) = v^-(0, t_{j+1}), V^{-(j+1)}(x_{\frac{N}{2}}) = v^-(d-, t_{j+1}), & \\ \mathcal{L}_h^{N,M} V^{+(j+1)}(x_i) = g(x_i, t_{j+1}), & \text{for all } (x_i, t_{j+1}) \in \Omega^{N+}, \\ V^{+(j+1)}(x_{\frac{N}{2}}) = v^+(d+, t_{j+1}), V^{+(j+1)}(x_N) = v^-(1, t_{j+1}). & \end{array}\right\} \tag{11}$$

The discrete singular components $W_l^{j+1}(x_i)$ and $W_r^{j+1}(x_i)$ are also decomposed as

$$W_l^{j+1}(x_i) = \begin{cases} W_l^{-(j+1)}(x_i), & (x_i, t_{j+1}) \in \Omega^{N-}, \\ W_l^{+(j+1)}(x_i), & (x_i, t_{j+1}) \in \Omega^{N+}, \end{cases}$$

$$W_r^{j+1}(x_i) = \begin{cases} W_r^{-(j+1)}(x_i), (x_i, t_{j+1}) \in \Omega^{N-}, \\ W_r^{+(j+1)}(x_i), (x_i, t_{j+1}) \in \Omega^{N+}, \end{cases}$$

where $W_l^{-(j+1)}(x_i), W_l^{+(j+1)}(x_i)$ approximates the layer components $w_l^-(x_i, t_{j+1})$ and $w_l^+(x_i, t_{j+1})$ and $W_r^{-(j+1)}(x_i), W_r^{+(j+1)}(x_i)$ approximates the layer components $w_r^-(x_i, t_{j+1})$ and $w_r^+(x_i, t_{j+1})$, respectively. These components satisfy the following equations:

$$\left.\begin{array}{l}\mathcal{L}_h^{N,M} W_l^{-(j+1)}(x_i)=0, \qquad \text{for all } (x_i,t_{j+1})\in\Omega^{N-},\\ W_l^{-(j+1)}(x_0)=w_l^-(0,t_{j+1}), W_l^{-(j+1)}(x_{\frac{N}{2}})=w_l^-(d,t_{j+1}),\\ \mathcal{L}_h^{N,M} W_l^{+(j+1)}(x_i)=0, \qquad \text{for all } (x_i,t_{j+1})\in\Omega^{N+},\\ W_l^{+(j+1)}(x_{\frac{N}{2}})=w_l^+(d,t_{j+1}), W_l^{+(j+1)}(x_N)=0.\end{array}\right\} \tag{12}$$

$$\left.\begin{array}{l}\mathcal{L}_h^{N,M} W_r^{-(j+1)}(x_i)=0, \qquad \text{for all } (x_i,t_{j+1})\in\Omega^{N-},\\ W_r^{-(j+1)}(x_0)=0, W_r^{-(j+1)}(x_{\frac{N}{2}})=w_r^-(d,t_{j+1}),\\ \mathcal{L}_h^{N,M} W_r^{+(j+1)}(x_i)=0, \qquad \text{for all } (x_i,t_{j+1})\in\Omega^{N+},\\ W_r^{+(j+1)}(x_{\frac{N}{2}})=w_r^+(d+,t_{j+1}), W_r^{+(j+1)}(x_N)=w_r(1,t_{j+1}).\end{array}\right\} \tag{13}$$

Hence, the complete discrete solution $U^{j+1}(x_i)$ is defined by

$$U^{j+1}(x_i)=\begin{cases}(V^{-(j+1)}+W_l^{-(j+1)}+W_r^{-(j+1)})(x_i), & (x_i,t_{j+1})\in\Omega^{N-},\\ (V^{-(j+1)}+W_l^{-(j+1)}+W_r^{-(j+1)})(d-) & \\ =(V^{+(j+1)}+W_l^{+(j+1)}+W_r^{+(j+1)})(d+), & (x_i,t_{j+1})=(d,t_{j+1}),\\ (V^{+(j+1)}+W_l^{+(j+1)}+W_r^{+(j+1)})(x_i), & (x_i,t_{j+1})\in\Omega^{N+}.\end{cases}$$

Lemma 7. Suppose that a mesh function $Y(x_i,t_j)$ satisfies $Y(x_i,t_j)\geq 0$, for all $(x_i,t_j)\in\Gamma_c^N$ and $\mathcal{L}_t^{N,M}Y(x_{N/2})\leq 0$ for all $j=0,\dots,M$. If $\mathcal{L}_h^{N,M}Y(x_i,t_j)\leq 0$ for all $(x_i,t_j)\in\Omega^{N-}\cup\Omega^{N+}$, then $Y(x_i,t_j)\geq 0$, for all $(x_i,t_j)\in\bar{\Omega}^{N,M}$.

Proof. The condition (10) ensures that the matrix generated by $\mathcal{L}_h^{N,M}$ satisfies $r_i^->0$, $r_i^+>0$ and $r_i^-+r_i^c+r_i^+<0$ in layer regions. For the case when $\sqrt{\alpha}\mu\leq\sqrt{\rho\epsilon}$, the operator $\mathcal{L}_c^{N,M}$ is used in the region $(\tau_1,d-\tau_2)$ and $(d+\tau_3,1-\tau_4)$ except transition points with $\mu h_k\|a\|\leq 2\epsilon$, where $k=2,5$ to guarantee $r_i^->0$ and $r_i^+>0$.

In the case when $\sqrt{\alpha}\mu\leq\sqrt{\rho\epsilon}$, the operator $\mathcal{L}_m^{N,M}$ is applied in the region $(\tau_1,d-\tau_2)$ and $(d+\tau_3,1-\tau_4)$ with $\left(\|b\|+\frac{2}{\Delta t}\right)h_k<2\mu\alpha,\ k=2,5$, otherwise $\mathcal{L}_u^{N,M}$ is used. At the transition point, $\mathcal{L}_m^{N,M}$ is applied with $\left(\|b\|+\frac{2}{\Delta t}\right)h_k<2\mu\alpha,\ k=2,3,5,6$, otherwise $\mathcal{L}_u^{N,M}$ is used to guarantee $r_i^->0$ and $r_i^+>0$. At the point of discontinuity, the operator $\mathcal{L}_t^{N,M}$ is used with $\left(\|b\|+\frac{2}{\Delta t}\right)h_k<2\mu\alpha,\ k=3,4$. The associated matrix with the operator $\mathcal{L}_h^{N,M}U^{j+1}(x_i)$ is negative of an M-matrix. The finite difference method is monotone and hence the finite difference operator satisfies the discrete minimum principle. □

Lemma 8. If $U(x_i, t_{j+1}), (x_i, t_{j+1}) \in \bar{\Omega}^{N,M}$ is a mesh function satisfying the difference scheme (8), then $\|U\|_{\bar{\Omega}^{N,M}} \leq C$.

Proof. Define the mesh function $\psi(x_i, t_{j+1}) = \phi(x_i, t_{j+1}) \pm U(x_i, t_{j+1})$, where $\phi(x_i, t_{j+1}) = \max\left\{|U^{j+1}(0)|, |U^{j+1}(1)|, \frac{\|g\|_{\bar{\Omega}^{N,M}}}{\beta}\right\}$. Clearly $\psi(x_i, t_{j+1}) \geq 0$ for all $(x_i, t_{j+1}) \in \Gamma_c^N$ and $\mathcal{L}_h^{N,M}\psi(x_i, t_{j+1}) = \mathcal{L}_h^{N,M}\phi(x_i, t_{j+1}) \pm \mathcal{L}_h^{N,M}U(x_i, t_{j+1}) \leq 0$.

At the point of discontinuity, we have

$$\mathcal{L}_t^{N,M}\psi(x_{\frac{N}{2}}, t_{j+1}) = \mathcal{L}_t^{N,M}\phi(x_{\frac{N}{2}}, t_{j+1}) \pm \mathcal{L}_t^{N,M}U(x_{\frac{N}{2}}, t_{j+1}) \leq 0.$$

Therefore, $\psi(x_i, t_{j+1}) \geq 0$, for all $(x_i, t_{j+1}) \in \bar{\Omega}^{N,M}$. This leads to the required result

$$\|U\|_{\bar{\Omega}^{N,M}} \leq C$$

□

4 Truncation error analysis

Lemma 9. The singular component $W_l^-(x_i, t_{j+1}), W_l^+(x_i, t_{j+1}), W_r^-(x_i, t_{j+1})$ and $W_r^+(x_i, t_{j+1})$ satisfy the following bounds:

$$|W_l^-(x_i, t_{j+1})| \leq C\gamma_{l,i}^-, \quad \gamma_{l,i}^- = \prod_{n=1}^{i}(1+\theta_2 h_n)^{-1}, \quad \gamma_{l,0}^- = C_1,\ i = 0, 1, \ldots, \frac{N}{2},$$

$$|W_l^+(x_i, t_{j+1})| \leq C\gamma_{l,i}^+, \quad \gamma_{l,i}^+ = \prod_{n=\frac{N}{2}+1}^{i}(1+\theta_1 h_n)^{-1}, \quad \gamma_{l,\frac{N}{2}}^+ = C_1,\ i = \frac{N}{2}+1, \ldots, N,$$

$$|W_r^-(x_i, t_{j+1})| \leq C\gamma_{r,i}^-, \quad \gamma_{r,i}^- = \prod_{n=i+1}^{\frac{N}{2}}(1+\theta_1 h_n)^{-1}, \quad \gamma_{r,\frac{N}{2}}^- = C_1,\ i = 0, 1, \ldots, \frac{N}{2},$$

$$|W_r^+(x_i, t_{j+1})| \leq C\gamma_{r,i}^+, \quad \gamma_{r,i}^+ = \prod_{n=i+1}^{N}(1+\theta_2 h_n)^{-1}, \quad \gamma_{r,N}^+ = C_1,\ i = \frac{N}{2}+1, \ldots, N.$$

Proof. Define the barrier function for the left layer term as

$$\eta_{l,i}^{-(j+1)} = C\gamma_{l,i}^{-(j+1)} \pm W_l^{-(j+1)}(x_i), \quad 0 \leq i \leq \frac{N}{2},\ 0 \leq j \leq M-1,$$

where

$$\gamma_{l,i}^{-(j+1)} = \begin{cases} \prod_{k=1}^{i}(1+\theta_2 h_k)^{-1}, \ 1 \le i \le \frac{N}{2}, \\ 1, \qquad\qquad\qquad\qquad i = 0. \end{cases}$$

For the both cases when $\sqrt{\alpha}\mu \le \sqrt{\rho\epsilon}$ and $\sqrt{\alpha}\mu > \sqrt{\rho\epsilon}$, for large enough C, $\eta_{l,0}^{-(j+1)} \ge 0, \eta_{r,i}^{-(0)} \ge 0$ and $\eta_{l,N/2}^{-(j+1)} \ge 0$.

Now,

$$\begin{aligned}\mathcal{L}_c^{N,M}\eta_{l,i}^{-(j+1)} &= \mathcal{L}_c^{N,M}\gamma_{l,i}^{-(j+1)} \pm \mathcal{L}_c^{N,M}W_l^{-(j+1)}(x_i) \\ &= \gamma_{l,i+1}^{-(j+1)}\Big(2\epsilon\theta_2^2\big(\frac{h_{i+1}}{h_{i+1}+h_i}-1\big) + 2\epsilon\theta_2^2 - \mu a^{j+\frac{1}{2}}(x_i)\theta_2 \\ &\qquad -\mu a^{j+\frac{1}{2}}(x_i)\theta_2^2\frac{h_i h_{i+1}}{h_i+h_{i+1}} - b^{j+\frac{1}{2}}(x_i)\Big).\end{aligned}$$

On simplification, we get

$$\begin{aligned}\mathcal{L}_c^{N,M}\eta_{l,i}^{-(j+1)} &\le \gamma_{l,i+1}^{-(j+1)}\Big(2\epsilon\theta_2^2 - \mu a^{j+\frac{1}{2}}(x_i)\theta_2 - b^{j+\frac{1}{2}}(x_i)\Big) \\ &\le \gamma_{l,i+1}^{-(j+1)}(\rho|a^{j+\frac{1}{2}}(x_i)| - b^{j+\frac{1}{2}}(x_i)) \le 0,\end{aligned}$$

$$\begin{aligned}\mathcal{L}_m^{N,M}\eta_{l,i}^{-(j+1)} &\le \gamma_{l,i+1}^{-(j+1)}\Big(2\epsilon\theta_2^2 - \mu \bar{a}^{j+\frac{1}{2}}(x_i)\theta_2 - \bar{b}^{j+\frac{1}{2}}(x_i)\Big) \\ &\le \gamma_{l,i+1}^{-(j+1)}(\rho|\bar{a}^{j+\frac{1}{2}}(x_i)| - \bar{b}^{j+\frac{1}{2}}(x_i)) \le 0,\end{aligned}$$

$$\begin{aligned}\mathcal{L}_u^{N,M}\eta_{l,i}^{-(j+1)} &\le \gamma_{l,i+1}^{-(j+1)}\Big(2\epsilon\theta_2^2 - \mu a^{j+\frac{1}{2}}(x_i)\theta_2 - b^{j+\frac{1}{2}}(x_i)\Big) \\ &\le \gamma_{l,i+1}^{-(j+1)}(\rho|a^{j+\frac{1}{2}}(x_i)| - b^{j+\frac{1}{2}}(x_i)) \le 0.\end{aligned}$$

By the discrete minimum principle for the continuous case [18], we obtain

$$\eta_{l,i}^{-(j+1)} \ge 0 \implies |W_l^{-(j+1)}(x_i)| \le C\prod_{k=1}^{i}(1+\theta_2 h_k)^{-1}, \quad 1 \le i \le \frac{N}{2}, \ 0 \le j \le M-1.$$

Similarly, we prove the bound for $W_l^{+(j+1)}(x_i)$ for $\frac{N}{2}+1 \le i \le N-1, \ 0 \le j \le M-1$.

Now, to prove the bound for $W_r^{-(j+1)}(x_i)$, we define the barrier function for the right layer component as

$$\eta_{r,i}^{-(j+1)} = C\gamma_{r,i}^{-(j+1)} \pm W_r^{-(j+1)}(x_i), \quad 0 \le i \le \frac{N}{2},\ 0 \le j \le M-1,$$

where

$$\gamma_{r,i}^{-(j+1)} = \begin{cases} \prod_{k=i+1}^{\frac{N}{2}} (1+\theta_1 h_k)^{-1}, 0 \le i < \frac{N}{2}, \\ 1, \qquad\qquad i = \frac{N}{2}. \end{cases}$$

For large enough C, we have $\eta_{r,0}^{-(j+1)} \ge 0, \eta_{r,i}^{-(0)} \ge 0$ and $\eta_{r,N/2}^{-(j+1)} \ge 0$.
Now,

$$\begin{aligned}
\mathcal{L}_c^{N,M}\eta_{r,i}^{-(j+1)} &= \mathcal{L}_c^{N,M}\gamma_{r,i}^{-(j+1)} \pm \mathcal{L}_c^{N,M}W_r^{-(j+1)}(x_i) \\
&= \frac{\gamma_{r,i}^{-(j+1)}}{1+\theta_1 h_i}\Bigg(2\epsilon\theta_1^2\big(\frac{h_i}{h_{i+1}+h_i}-1\big) + 2\epsilon\theta_1^2 + \mu a^{j+\frac{1}{2}}(x_i)\theta_1 \\
&\quad + \frac{\theta_1^2\mu a^{j+\frac{1}{2}}(x_i)h_{i+1}}{h_i+h_{i+1}} - b^{j+\frac{1}{2}}(x_i)\Bigg) \\
&\le \frac{\gamma_{r,i}^{-(j+1)}}{1+\theta_1 h_i}\left(2\epsilon\theta_1^2 + \mu a^{j+\frac{1}{2}}(x_i)\theta_1 - b^{j+\frac{1}{2}}(x_i)\right), \quad \text{as } \frac{h_{i+1}}{h_{i+1}+h_i} - 1 \le 0.
\end{aligned}$$

For the case when $\sqrt{\alpha}\mu \le \sqrt{\rho\epsilon}$, on simplification, we get

$$\mathcal{L}_c^{N,M}\eta_{r,i}^{-(j+1)} \le \frac{\gamma_{r,i}^{-(j+1)}}{1+\theta_1 h_i}\left(\rho|a^{j+\frac{1}{2}}(x_i)| - b^{j+\frac{1}{2}}(x_i)\right) \le 0,$$

$$\mathcal{L}_m^{N,M}\eta_{r,i}^{-(j+1)} \le \frac{\gamma_{r,i}^{-}}{1+\theta_1 h_i}\left((\rho|\bar{a}^{j+\frac{1}{2}}(x_i)| - \bar{b}^{j+\frac{1}{2}}(x_i))\right) \le 0,$$

$$\mathcal{L}_u^{N,M}\eta_{r,i}^{-(j+1)} \le \frac{\gamma_{r,i}^{-}}{1+\theta_1 h_i}\left((\rho|a^{j+\frac{1}{2}}(x_i)| - b^{j+\frac{1}{2}}(x_i))\right) \le 0,$$

and for the case when $\sqrt{\alpha}\mu > \sqrt{\rho\epsilon}$,

$$\mathcal{L}_c^{N,M}\eta_{r,i}^{-(j+1)} \le \frac{\gamma_{r,i}^{-(j+1)}}{1+\theta_1 h_i}\left(\frac{\alpha\mu^2}{2\epsilon}(\alpha + a^{j+\frac{1}{2}}(x_i)) - b^{j+\frac{1}{2}}(x_i)\right) \le 0,$$

$$\mathcal{L}_m^{N,M}\eta_{r,i}^{-(j+1)} \le \frac{\gamma_{r,i}^{-}}{1+\theta_1 h_i}\left(\frac{\alpha\mu^2}{2\epsilon}(\alpha + \bar{a}^{j+\frac{1}{2}}(x_i)) - \bar{b}^{j+\frac{1}{2}}(x_i))\right) \le 0,$$

$$\mathcal{L}_u^{N,M}\eta_{r,i}^{-(j+1)} \leq \frac{\gamma_{r,i}^{-}}{1+\theta_1 h_i}\left(\frac{\alpha\mu^2}{2\epsilon}(\alpha + a^{j+\frac{1}{2}}(x_i)) - b^{j+\frac{1}{2}}(x_i))\right) \leq 0.$$

By the discrete minimum principle for the continuous case [18], we obtain

$$\eta_{r,i}^{-(j+1)} \geq 0 \implies |W_r^{-(j+1)}(x_i)| \leq C\prod_{k=i+1}^{N/2}(1+\theta_1 h_k)^{-1}, \quad 1 \leq i \leq \frac{N}{2},\ 0 \leq j \leq M-1.$$

Similarly, we prove the bound for $W_r^{+(j+1)}(x_i)$ for $\frac{N}{2}+1 \leq i \leq N-1,\ 0 \leq j \leq M-1$. □

For the truncation error at the mesh point $(x_i, t_{j+1}) \in \Omega^{N,M}\backslash\{d\}$, when mesh is arbitrary, we have

$$|\mathcal{L}_h^{N,M}(e(x_i))| \leq \begin{cases} |(\mathcal{L}_c^{N,M} - \mathcal{L})y_i| \leq \epsilon\hbar_i\|y_{xxx}\| + \mu\hbar_i\|a\|\|y_{xx}\| + \|y_{tt}\| \\ |(\mathcal{L}_m^{N,M} - \mathcal{L})y_i| \leq \epsilon\hbar_i\|y_{xxx}\| + C\mu h_{i+1}^2(\|y_{xxx}\| + \|y_{xx}\|) + \|y_{tt}\| \\ |(\mathcal{L}_u^{N,M} - \mathcal{L})y_i| \leq \epsilon\hbar_i\|y_{xxx}\| + \mu h_{i+1}\|a\|\|y_{xx}\| + \|y_{tt}\|. \end{cases}$$

On a uniform mesh with step size h, we get

$$|\mathcal{L}_h^{N,M}(e(x_i))| \leq \begin{cases} |(\mathcal{L}_c^{N,M} - \mathcal{L})y_i| \leq \epsilon h^2\|y_{xxxx}\| + \mu h^2|a\|\|y_{xxx}\| + \|y_{tt}\| \\ |(\mathcal{L}_m^{N,M} - \mathcal{L})y_i| \leq \epsilon h\|y_{xxx}\| + C\mu h_{i+1}^2(\|y_{xxx}\| + \|y_{xx}\|) + \|y_{tt}\| \\ |(\mathcal{L}_u^{N,M} - \mathcal{L})y_i| \leq \epsilon h^2\|y_{xxxx}\| + \mu h\|a\|\|y_{xx}\| + \|y_{tt}\|, \end{cases}$$

where $C_{\|a\|,\|a'\|}$ is a positive constant depending on $\|a\|$ and $\|a'\|$.

Lemma 10. The discrete regular component $V^{j+1}(x_i)$ defined in (11) and $v(x,t)$ is solution of the problem (2). So, the error in the regular component satisfies the following estimate for $\sqrt{\alpha}\mu \leq \sqrt{\rho\epsilon}$:

$$\|V - v\|_{\Omega^{N-}\cup\Omega^{N+}} \leq C(N^{-2} + \Delta t^2).$$

Proof. For the regular part of the solution $y(x,t)$ of (1) for the case where $\sqrt{\alpha}\mu \leq \sqrt{\rho\epsilon}$ and when mesh is uniform ($\tau_1 = \tau_2 = \frac{d}{4}$) in the domain $(x_i, t_{j+1}) \in \Omega^{N-}$, the truncation error is

$$\begin{aligned} |\mathcal{L}_h^{N,M}(V^{-(j+1)} - v^{-(j+1)})(x_i)| &= |\mathcal{L}_c^{N,M}(V^{-(j+1)} - v^{-(j+1)})(x_i)| \\ &\leq \left|\epsilon\left(\delta^2 - \frac{d^2}{dx^2}\right)v^{-(j+1)}(x_i)\right| \end{aligned}$$

$$
\begin{aligned}
&+\mu|a^{j+\frac{1}{2}}(x_i)|\left|\left(D^0-\frac{d}{dx}\right)v^{-(j+1)}(x_i)\right| \\
&+\left|\left(D_t^- - \frac{\delta}{\delta t}\right)v^{-(j+1)}(x_i)\right| \\
&\leq \epsilon h^2\|v^-_{xxxx}\| + \mu h^2\|a\|\|v^-_{xxx}\| + C_1\Delta t^2 \\
&\leq C(N^{-2}+\Delta t^2).
\end{aligned}
$$

When mesh is nonuniform in $(x_i, t_{j+1}) \in \Omega^{N-}$ for $\sqrt{\alpha}\mu \leq \sqrt{\rho\epsilon}$:

$$
|\mathcal{L}_c^{N,M}(V^{-(j+1)}-v^{-(j+1)})(x_i)| \leq \epsilon\hbar_i\|v^-_{xxx}\| + \mu\hbar_i\|a\|\|v^-_{xx}\| + C_1\Delta t^2 \leq C(N^{-2}+\Delta t^2).
$$

For the case where $\sqrt{\alpha}\mu > \sqrt{\rho\epsilon}$ and when mesh is uniform ($\tau_1 = \tau_2 = \frac{d}{4}$) in the domain $(x_i, t_{j+1}) \in \Omega^{N-}$:

$$
|\mathcal{L}_h^{N,M}(V^{-(j+1)}-v^{-(j+1)})(x_i)| \leq C(N^{-2}+\Delta t^2).
$$

When mesh is nonuniform:

$$
\begin{aligned}
|\mathcal{L}_c^{N,M}(V^{-(j+1)}-v^{-(j+1)})(x_i)| &\leq \epsilon\hbar_i\|v^-_{xxx}\| + \mu\hbar_i\|a\|\|v^-_{xx}\| + C_1\Delta t^2 \\
&\leq C(N^{-2}+\Delta t^2),
\end{aligned}
$$

$$
\begin{aligned}
|\mathcal{L}_m^{N,M}(V^{-(j+1)}-v^{-(j+1)})(x_i)| &\leq \epsilon\hbar_i\|v^-_{xxx}\| + C\mu h_{i+1}^2(\|v^-_{xxx}\| + \|v^-_{xx}\|) \\
&\leq C(N^{-2}+\Delta t^2),
\end{aligned}
$$

$$
\begin{aligned}
|\mathcal{L}_u^{N,M}(V^{-(j+1)}-v^{-(j+1)})(x_i)| &\leq \epsilon\hbar_i\|v^-_{xxx}\| + C\mu h_{i+1}(\|v^-_{xx}\|) \\
&\leq C(N^{-2}+\Delta t^2).
\end{aligned}
$$

At the transition point τ_1:

$$
|\mathcal{L}_m^{N,M}(V^{-(j+1)}-v^{-(j+1)})(x_i)| \leq C(N^{-2}+\Delta t^2).
$$

Define the barrier function in $(x_i, t_{j+1}) \in \Omega^{N-}$:

$$
\psi^{j+1}(x_i) = C(N^{-2}+\Delta t^2) \pm (V^{-(j+1)}-v^{-(j+1)})(x_i).
$$

For large C, $\psi^{j+1}(0) \geq 0,\ \psi^{j+1}(x_{\frac{N}{2}}) \geq 0, \psi^0(x_i) \geq 0$ and $\mathcal{L}_h^{N,M}\psi^{j+1}(x_i) \leq 0$. Hence, using the approach given in [8], we get $\psi^{j+1}(x_i) \geq 0$ and

$$|(V^{-(j+1)} - v^{-(j+1)})(x_i)|_{\Omega^{N-}} \leq C(N^{-2} + \Delta t^2). \tag{14}$$

Similarly, we can estimate the error bounds for right regular part in the domain $(x_i, t_{j+1}) \in \Omega^{N+}$:

$$|(V^{+(j+1)} - v^{+(j+1)})(x_i)|_{\Omega^{N+}} \leq C(N^{-2} + \Delta t^2). \tag{15}$$

Combining the above results (14) and (15), we obtain

$$\|V - v\|_{\Omega^{N-} \cup \Omega^{N+}} \leq C(N^{-2} + \Delta t^2).$$

□

Lemma 11. Let $W_l(x_i, t_{j+1}), w_l(x,t)$ be solution of the problem (12) and (3), respectively. The left singular component of the truncation error satisfies the following estimate:

$$|\|W_l - w_l\|_{\Omega^{N-} \cup \Omega^{N+}} \leq \begin{cases} C((N^{-1}\ln N)^2 + \Delta t^2), & \sqrt{\alpha}\mu \leq \sqrt{\rho\epsilon}, \\ C(N^{-2}(\ln N)^3 + \Delta t^2), & \sqrt{\alpha}\mu > \sqrt{\rho\epsilon}. \end{cases} \tag{16}$$

Proof. The truncation error in case of uniform ($\tau_1 = \tau_2 = \frac{d}{4}$) for the case $\sqrt{\alpha}\mu \leq \sqrt{\rho\epsilon}$ in the domain $(x_i, t_{j+1}) \in \Omega^{N-}$ is

$$\begin{aligned} |\mathcal{L}_c^{N,M}(W_l^{-(j+1)} - w_l^{-(j+1)})(x_i)| &\leq CN^{-2}(\epsilon\|w_{l,xxxx}^{-(j+1}\| + \mu\|w_{l,xxx}^{-(j+1)}\|) + C_1\Delta t^2\|w_{tt}\| \\ &\leq C(N^{-2}(\ln N)^2 + \Delta t^2). \end{aligned}$$

In the case of nonuniform mesh, we split the argument into two parts. For $(x_i, t_{j+1}) \in [\tau_1, d) \times (0, T]$ from Lemma 5, we obtain

$$|w_l^{-(j+1)}(x_i)| \leq C\exp^{-\theta_2 x_i} \leq C\exp^{-\theta_2\tau_1} \leq CN^{-2}. \tag{17}$$

Also, from Lemma 9, we have

$$|W_l^{-(j+1)}(x_i)| \leq C\prod_{k=1}^{\frac{N}{8}}(1 + \theta_2 h_k)^{-1} \leq \left(1 + \frac{16\ln N}{N}\right)^{-N/8} \leq CN^{-2}.$$

Hence, for all $(x_i, t_{j+1}) \in [\tau_1, d) \times (0, T]$, we have

$$|(W_l^{-(j+1)} - w_l^{-(j+1)})(x_i)| \leq |W_l^{-(j+1)}(x_i)| + |w_l^{-(j+1)}(x_i)| \leq CN^{-2}.$$

For $\sqrt{\alpha}\mu \leq \sqrt{\rho\epsilon}$, the truncation error for the left layer component in the inner region $(0,\tau_1)\times(0,T]$, is

$$|\mathcal{L}_c^{N,M}(W_l^{-(j+1)} - w_l^{-(j+1)})(x_i)| \leq C(N^{-2}(\ln N)^2 + \Delta t^2).$$

We choose the barrier function for the layer component as

$$\psi^{j+1}(x_i) = C_1((N^{-1}\ln N)^2 + \Delta t^2) \pm (W_l^{-(j+1)} - w_l^{-(j+1)})(x_i), \qquad (x_i,t_{j+1}) \in \Omega^{N-}.$$

For sufficiently large C, we have $\psi^{j+1}(x_0) \geq 0, \psi^{j+1}(x_{N/8}) \geq 0, \psi^0(x_i) \geq 0$ and $\mathcal{L}_c^{N,M}\psi^{j+1}(x_i) \leq 0$. Hence by the discrete maximum principle in [18], $\psi^{j+1}(x_i) \geq 0$. So, we can obtain the following bounds:

$$|(W_l^{-(j+1)} - w_l^{-(j+1)})(x_i)| \leq C(N^{-2}(\ln N)^2 + \Delta t^2), \quad \text{for all } (x_i,t_{j+1}) \in \Omega^{N-}.$$

For the case where $\sqrt{\alpha}\mu > \sqrt{\rho\epsilon}$ and when the mesh is uniform $(\tau_1 = \tau_2 = \frac{d}{4})$ in $(x_i,t_{j+1}) \in \Omega^{N-}$:

$$|\mathcal{L}_h^{N,M}(W_l^{-(j+1)} - w_l^{-(j+1)})(x_i)| \leq C(N^{-2}(\ln N)^3 + \Delta t^2).$$

The truncation error for the left layer component in the inner region $(0,\tau_1)\times(0,T]$, when mesh is nonuniform is

$$|\mathcal{L}_c^{N,M}(W_l^{-(j+1)} - w_l^{-(j+1)})(x_i)| \leq CN^{-2}(\ln N)^3 + C_1\Delta t^2,$$

$$\begin{aligned}|\mathcal{L}_m^{N,M}(W_l^{-(j+1)} - w_l^{-(j+1)})(x_i)| &\leq Ch_1\epsilon\|w_{l,xxx}^-\| + Ch_1^2\mu(\|w_{l,xxx}^-\| + \|w_{l,xx}^-\|) + C_1\Delta^2\\ &\leq Ch_1^2\mu(\|w_l^{-(3)}\| + \|w_l^{-(2)}\|) + C_1\Delta t^2\\ &\leq C(N^{-2}(\ln N)^3 + \Delta t^2),\end{aligned}$$

$$|\mathcal{L}_u^{N,M}(W_l^{-(j+1)} - w_l^{-(j+1)})(x_i)| \leq C(N^{-2}(\ln N)^3 + \Delta t^2).$$

We choose the barrier function for the layer component as

$$\psi^{j+1}(x_i) = C_1((N^{-1}\ln N)^3 + \Delta t^2) \pm (W_l^{-(j+1)} - w_l^{-(j+1)})(x_i),\ (x_i,t_{j+1})) \in \Omega^{N-}.$$

For sufficiently large C, we have $\psi^{j+1}(x_0) \geq 0, \psi^{j+1}(x_{N/8}) \geq 0, \psi^0(x_i) \geq 0$ and $\mathcal{L}_h^{N,M}\psi^{j+1}(x_i) \leq 0$. Hence by the discrete maximum principle in [18], $\psi^{j+1}(x_i) \geq 0$. So, we can obtain the following bounds in $(0,d)\times(0,T]$:

$$|(W_l^{-(j+1)} - w_l^{-(j+1)})(x_i)| \leq \begin{cases} C((N^{-1}\ln N)^2 + \Delta t^2), & \sqrt{\alpha}\mu \leq \sqrt{\rho\epsilon}, \\ C(N^{-2}(\ln N)^3 + \Delta t^2), & \sqrt{\alpha}\mu > \sqrt{\rho\epsilon}. \end{cases} \tag{18}$$

By a similar argument in the domain $(d, 1) \times (0, T]$, we have

$$|(W_l^{+(j+1)} - w_l^{+(j+1)})(x_i)| \leq \begin{cases} C((N^{-1}\ln N)^2 + \Delta t^2), & \sqrt{\alpha}\mu \leq \sqrt{\rho\epsilon}, \\ C(N^{-2}(\ln N)^3 + \Delta t^2), & \sqrt{\alpha}\mu > \sqrt{\rho\epsilon}. \end{cases} \tag{19}$$

Combining the results (18) and (19), the desired result is obtained. □

Lemma 12. Let $W_r^-(x_i, t_{j+1}), w_r^-(x, t)$ be solution of the problem (13) and (4), respectively. The right singular component of the truncation error satisfies the following estimate:

$$\|W_r - w_r\|_{\Omega^{N-} \cup \Omega^{N+}} \leq \begin{cases} C((N^{-1}\ln N)^2 + \Delta t^2), & \sqrt{\alpha}\mu \leq \sqrt{\rho\epsilon}, \\ C(N^{-2}(\ln N)^3 + \Delta t^2), & \sqrt{\alpha}\mu > \sqrt{\rho\epsilon}. \end{cases} \tag{20}$$

Proof. The truncation error for $\sqrt{\alpha}\mu \leq \sqrt{\rho\epsilon}$, when the mesh is uniform ($\tau_1 = \tau_2 = \frac{d}{4}$) in $(x_i, t_{j+1}) \in \Omega^{N-}$ is

$$\begin{aligned} |\mathcal{L}_c^{N,M}(W_r^{-(j+1)} - w_r^{-(j+1)})(x_i)| &\leq CN^{-2}(\epsilon\|w^-_{l,xxxx}\| + \mu\|w^-_{r,xxx}\|) + C_1\Delta t^2 \\ &\leq C(N^{-2}(\ln N)^2 + \Delta t^2). \end{aligned}$$

In case of nonuniform mesh, we split the interval $(0, d) \times (0, T]$ into two parts $(0, d - \tau_2] \times (0, T]$ and $(d - \tau_2, d) \times (0, T]$.

In the domain $(x_i, t_{j+1}) \in (0, d - \tau_2] \times (0, T]$, we have

$$|w_r^{-(j+1)}(x_i)| \leq C \exp^{-\theta_1(d-x_i)} \leq C \exp^{-\theta_1\tau_2} \leq CN^{-2}. \tag{21}$$

Also, from Lemma 9,

$$|W_r^{-(j+1)}(x_i)| \leq C \prod_{k=1}^{\frac{N}{8}} (1 + \theta_1 h_k)^{-1} \leq \left(1 + \frac{16\ln N}{N}\right)^{-N/8} \leq CN^{-2}.$$

Hence, for all $(x_i, t_{j+1}) \in (0, d - \tau_2] \times (0, T]$, we have

$$|(W_r^{-(j+1)} - w_r^{-(j+1)})(x_i)| \leq |W_r^{-(j+1)}(x_i)| + |w_r^{-(j+1)}(x_i)| \leq CN^{-2}.$$

For $\sqrt{\alpha}\mu \leq \sqrt{\rho\epsilon}$, the truncation error for the left layer component in the inner region $(d-\tau_2, d) \times (0, T]$, is

$$|\mathcal{L}_c^{N,M}(W_r^{-(j+1)} - w_r^{-(j+1)})(x_i)| \leq C(N^{-2}(\ln N)^2 + \Delta t^2).$$

We choose the barrier function for the layer component as

$$\psi^{j+1}(x_i) = C_1((N^{-1}\ln N)^2 + \Delta t^2) \pm (W_r^{-(j+1)} - w_r^{-(j+1)})(x_i), \qquad (x_i, t_{j+1}) \in \Omega^{N-}.$$

For sufficiently large C_1, we have $\psi^{j+1}(x_{\frac{3N}{8}}) \geq 0, \psi^{j+1}(x_{N/2}) \geq 0, \psi^0(x_i) \geq 0$ and $\mathcal{L}_h^{N,M}\psi^{j+1}(x_i) \leq 0$. Hence by the discrete maximum principle in [18], $\psi^{j+1}(x_i) \geq 0$. So, by using the discrete maximum principle, we can obtain the following bounds:

$$|(W_r^{-(j+1)} - w_r^{-(j+1)})(x_i)| \leq C(N^{-2}(\ln N)^2 + \Delta t^2), \qquad \text{for all } (x_i, t_{j+1}) \in \Omega^{N-}.$$

For $\sqrt{\alpha}\mu > \sqrt{\rho\epsilon}$, when mesh is uniform ($\tau_1 = \tau_2 = \frac{d}{4}$) in $(0, d) \times (0, T]$, we have

$$|\mathcal{L}_h^{N,M}(W_r^{-(j+1)} - w_r^{-(j+1)})(x_i)| \leq C(N^{-2}(\ln N)^3 + \Delta t^2).$$

In case of nonuniform mesh, the truncation error for the left layer component in the inner region $(d-\tau_2, d) \times (0, T]$, is

$$|\mathcal{L}_c^{N,M}(W_r^{-(j+1)} - w_r^{-(j+1)})(x_i)| \leq CN^{-2}(\ln N)^2 + C_1\Delta t^2.$$

We choose the barrier function for the layer component as

$$\psi^{j+1}(x_i) = C_1(N^{-2}\ln N^3 + \Delta t^2) \pm (W_r^{-(j+1)} - w_r^{-(j+1)})(x_i), \qquad (x_i, t_{j+1}) \in \Omega^{N-}.$$

For sufficiently large C_1, we have $\psi^{j+1}(x_{\frac{3N}{8}}) \geq 0, \psi^{j+1}(x_{N/2}) \geq 0, \psi^0(x_i) \geq 0$ and $\mathcal{L}_h^{N,M}\psi^{j+1}(x_i) \leq 0$. Hence by the discrete maximum principle in [18], $\psi^{j+1}(x_i) \geq 0$. So, by using the discrete maximum principle, we can obtain the following bounds in $(x_i, t_{j+1}) \in \Omega^{N-}$:

$$|(W_r^{-(j+1)} - w_r^{-(j+1)})(x_i)| \leq \begin{cases} C((N^{-1}\ln N)^2 + \Delta t^2), & \sqrt{\alpha}\mu \leq \sqrt{\rho\epsilon}, \\ C(N^{-2}(\ln N)^3 + \Delta t^2), & \sqrt{\alpha}\mu > \sqrt{\rho\epsilon}. \end{cases} \tag{22}$$

By a similar argument in the domains $(x_i, t_{j+1}) \in \Omega^{N+}$, we have

$$|(W_r^{+(j+1)} - w_r^{+(j+1)})(x_i)| \leq \begin{cases} C((N^{-1}\ln N)^2 + \Delta t^2), & \sqrt{\alpha}\mu \leq \sqrt{\rho\epsilon}, \\ C(N^{-2}(\ln N)^3 + \Delta t^2), & \sqrt{\alpha}\mu > \sqrt{\rho\epsilon}. \end{cases} \quad (23)$$

Combining the results (22) and (23), the desired result is obtained. □

Lemma 13. The error $e(x_{\frac{N}{2}}, t_{j+1})$ estimated at the point of discontinuity $(x_{\frac{N}{2}}, t_{j+1}) = (d, t_{j+1}), 0 \leq j \leq M-1$ satisfies the following estimates:

$$|\mathcal{L}_h^{N,M}(U-u)(x_{\frac{N}{2}}, t_{j+1})| \leq \begin{cases} \dfrac{Ch^2}{\epsilon^{3/2}}, & \sqrt{\alpha}\mu \leq \sqrt{\rho\epsilon}, \\ \dfrac{Ch^2\mu^3}{\epsilon^3}, & \sqrt{\alpha}\mu > \sqrt{\rho\epsilon}, \end{cases}$$

where $h = \max\{h_3, h_4\}$.

Proof. For $\sqrt{\alpha}\mu \leq \sqrt{\rho\epsilon}$, the truncation error at the point $x_{\frac{N}{2}} = d$ is

$$\begin{aligned} &\left|\mathcal{L}_h^{N,M} U^{j+1}(x_{N/2}) - \frac{2h_3^2 g_{N/2-1}^{j+1} h_4}{2\epsilon - h_3\mu a_{N/2-1}^{j+\frac{1}{2}}} - \frac{2h_4^2 g_{N/2+1}^{j+1} h_3}{2\epsilon + h_4\mu a_{N/2+1}^{j+\frac{1}{2}}}\right| \\ &\leq |\mathcal{L}_t^{N,M} U^{j+1}(x_{N/2})| \\ &\quad + \frac{2h_3^2 h_4}{2\epsilon - h_3\mu a_{N/2-1}^{j+\frac{1}{2}}} |\mathcal{L}_c^{N,M} u(x_{N/2-1}, t_{j+1}) - g_{N/2-1}^{j+1}| \\ &\quad + \frac{2h_4^2 h_3}{2\epsilon + h_4\mu a_{N/2+1}^{j+\frac{1}{2}}} |\mathcal{L}_c^{N,M} u(x_{N/2+1}, t_{j+1}) - g_{N/2+1}^{j+1}| \\ &\leq Ch^2 \|u_{xxx}\| \\ &\leq \frac{Ch^2}{\epsilon^{3/2}}. \end{aligned}$$

By using the bounds given in Lemma 4 for $\|u_{xxx}\|$, we get the above estimate. For $\sqrt{\alpha}\mu > \sqrt{\rho\epsilon}$, the truncation error at the point $x_{\frac{N}{2}} = \frac{d}{2}$ is

$$\begin{aligned} &\left|\mathcal{L}_h^{N,M} U^{j+1}(x_{N/2}) - \frac{2h_3^2 g_{N/2-1}^{j+\frac{1}{2}} h_4}{2\epsilon - h_3\mu a_{N/2-1}^{j+\frac{1}{2}}} - \frac{2h_4^2 g_{N/2+1}^{j+\frac{1}{2}} h_3}{2\epsilon + h_4\mu a_{N/2+1}^{j+\frac{1}{2}}}\right| \\ &\leq |\mathcal{L}_t^{N,M} U^{j+1}(x_{N/2})| \\ &\quad + \frac{2h_3^2 h_4}{2\epsilon - h_3\mu a_{N/2-1}^{j+\frac{1}{2}}} |\mathcal{L}_c^{N,M} u(x_{N/2-1}, t_{j+1}) - g_{N/2-1}^{j+1}| \end{aligned}$$

$$
\begin{aligned}
&+\frac{2h_4^2h_3}{2\epsilon+h_4\mu a_{N/2+1}^{j+\frac{1}{2}}}|\mathcal{L}_c^{N,M}u(x_{N/2+1},t_{j+1})-g_{N/2+1}^{j+1}| \\
&\le Ch^2\|u_{xxx}\| \\
&\le \frac{Ch^2\mu^3}{\epsilon^3}
\end{aligned}
$$

By using the bounds given in Lemma 4 for $\|u_{xxx}\|$, we get the above estimate.

□

Theorem 3. Let $u(x,t)$ and $U(x,t)$ be the solutions of (1) and (8), respectively. Then

$$\|U-u\|_{\bar{\Omega}^{N,M}} \le C(N^{-2}\ln N^3+\Delta t^2),$$

where C is a constant independent of ϵ,μ and discretization parameters N,M.

Proof. From Lemmas 10, 11 and 12, we have

$$\|U-u\|_{\Omega^{N-}\cup\Omega^{N+}} \le \begin{cases} C(N^{-2}(\ln N)^2+\Delta t^2), & \sqrt{\alpha}\mu\le\sqrt{\rho\epsilon}, \\ C(N^{-2}(\ln N)^3+\Delta t^2), & \sqrt{\alpha}\mu>\sqrt{\rho\epsilon}. \end{cases}$$

Let $\sqrt{\alpha}\mu \le \sqrt{\rho\epsilon}$. To find error at the point of discontinuity $x_{\frac{N}{2}}=d$, we have considered the discrete barrier function $\phi_1(x_i,t_{j+1})=\psi_1(x_i,t_{j+1})\pm e(x_i,t_{j+1})$ defined in the interval $(d-\tau_2,d+\tau_3)\times(0,T]$, where

$$
\begin{aligned}
\psi_1(x_i,t_{j+1}) =& C(N^{-2}(\ln N)^3+\Delta t^2) \\
&+\frac{Ch^2}{\epsilon^{3/2}}\begin{cases} x_i-(d+\tau_2), & (x_i,t_{j+1})\in\Omega^{N,M}\cap(d-\tau_2,d)\times(0,T], \\ d-\tau_3-x_i, & (x_i,t_{j+1})\in\Omega^{N,M}\cap(d,d+\tau_3)\times(0,T]. \end{cases}
\end{aligned}
$$

For $x_i\in(d-\tau_2,d+\tau_3)$, $\phi_1(d-\tau_2,t_{j+1})$, $\phi_1(d+\tau_3,t_{j+1}),\phi_1(x_i,t_0)$ are nonnegative and $\mathcal{L}_h^{N,M}\phi_1(x_i,t_{j+1})\le 0$, for all $(x_i,t_{j+1})\in(d-\tau_2,d+\tau_3)\times(0,T]$. Also, $\mathcal{L}_t^{N,M}\phi_1(x_{N/2},t_{j+1})\le 0$.

Hence, by applying the discrete minimum principle, we get $\phi_1(x_i,t_{j+1})\ge 0$.

Therefore, for $(x_i,t_{j+1})\in(d-\tau_2,d+\tau_3)\times(0,T]$, we have

$$|(U-u)(x_i,t_{j+1})|\le C_1(N^{-2}(\ln N)^3+\Delta t^2)+\frac{C_2h^2\tau}{\epsilon^{3/2}}\le C(N^{-2}(\ln N)^3+\Delta t^2). \tag{24}$$

For $\sqrt{\alpha}\mu > \sqrt{\rho\epsilon}$, consider the discrete barrier function $\phi_2(x_i, t_{j+1}) = \psi_2(x_i, t_{j+1}) \pm e(x_i, t_{j+1})$ defined in the interval $(d-\tau_2, d+\tau_3) \times (0, T]$, where

$$\begin{aligned}\psi_2(x_i, t_{j+1}) =& C(N^{-2}(\ln N)^3 + \Delta t^2) \\ &+ C_1 \frac{h^2\mu^3}{\epsilon^3} \begin{cases} x_i - (d+\tau_2), & (x_i, t_{j+1}) \in \Omega^{N,M} \cap (d-\tau_2, d) \times (0, T], \\ d - \tau_3 - x_i, & (x_i, t_{j+1}) \in \Omega^{N,M} \cap (d, d+\tau_3) \times (0, T]. \end{cases}\end{aligned}$$

We have $\phi_2(d-\tau_2, t_{j+1})$ and $\phi_2(d+\tau_3, t_{j+1}), \phi_2(x_i, t_0),\ x_i \in (d-\tau_2, d+\tau_3)$ are nonnegative and $\mathcal{L}_h^{N,M}\phi_2(x_i, t_{j+1}) \leq 0,$ for all $(x_i, t_{j+1}) \in (d-\tau_2, d+\tau_3) \times (0, T]$. Also, $\mathcal{L}_t^{N,M}\phi_2(x_i, t_{j+1}) \leq 0$.
Hence by applying the discrete minimum principle, we get $\phi_2(x_i, t_{j+1}) \geq 0$. Therefore, for $(x_i, t_{j+1}) \in (d-\tau_2, d+\tau_3) \times (0, T]$, we have

$$|(U-u)(x_i, t_{j+1})| \leq C(N^{-2}(\ln N)^3 + \Delta t^2). \tag{25}$$

By combining the result (24) and (25), we obtain the desired result. □

5 Numerical examples

To demonstrate the effectiveness of the proposed hybrid difference approach, we proposed a numerical method on three test problems with discontinuous convection coefficients and source terms. As the exact solutions to these problems are unknown, we used the double mesh method [7, 6] to evaluate the accuracy of the numerical approximations obtained. The double mesh difference is defined by

$$E^{N,M} = \max_j \left(\max_i |U_{2i,2j}^{2N,2M} - U_{i,j}^{N,M}| \right),$$

where $U_i^{N,M}$ and $U_{2i}^{2N,2M}$ are the solutions on the mesh $\bar{\Omega}^{N,M}$ and $\bar{\Omega}^{2N,2M}$, respectively. The order of convergence is given by

$$R^{N,M} = \log_2 \left(\frac{E^{N,M}}{E^{2N,2M}} \right).$$

We also compute the error and order of convergence by fixing ϵ and varying μ from a larger set, say $\mu \in S = \{10^{-j}, 2, 4, 6\}$ and name them as

$$E_\epsilon^{N,M} = \max_{\mu \in S} E^{N,M}.$$

The order of convergence is given by

$$R_\epsilon^{N,M} = \log_2 \left(\frac{E_\epsilon^{N,M}}{E_\epsilon^{2N,2M}} \right).$$

Example 1. Consider

$$(\epsilon u_{xx} + \mu a u_x - bu - u_t)(x,t) = f(x,t), \qquad (x,t) \in ((0,.5) \cup (0.5,1)) \times (0,1],$$

$$u(0,t) = u(1,t) = u(x,0) = 0,$$

with

$$a(x,t) = \begin{cases} -(1 + x(1-x)), & 0 \le x \le 0.5, t \in (0,1], \\ 1 + x(1-x), & 0.5 < x \le 1, t \in (0,1], \end{cases}$$

$$f(x,t) = \begin{cases} -2(1+x^2)t, & 0 \le x \le 0.5, t \in (0,1], \\ 2(1+x^2)t, & 0.5 < x \le 1, t \in (0,1], \end{cases}$$

and $b(x,t) = 1 + \exp(x)$.

Example 2. Consider

$$(\epsilon u_{xx} + \mu a u_x - bu - u_t)(x,t) = f(x,t), \qquad (x,t) \in ((0,0.5)) \cup (0.5,1)) \times (0,1],$$
$$u(0,t) = u(1,t) = u(x,0) = 0,$$

with

$$a(x,t) = \begin{cases} -(1 + x(1-x)), 0 \le x \le 0.5, t \in (0,1], \\ 1 + x(1-x), \quad 0.5 < x \le 1, t \in (0,1], \end{cases}$$

$$f(x,t) = \begin{cases} -2(1+x^2)t, 0 \le x \le 0.5, t \in (0,1], \\ 3(1+x^2)t, \quad 0.5 < x \le 1, t \in (0,1], \end{cases}$$

with and $b(x,t) = 1 + \exp(x)$.

Example 3. Consider

$$(\epsilon u_{xx} + \mu a u_x - bu - u_t)(x,t) = f(x,t), \qquad (x,t) \in ((0,.5) \cup (0.5,1)) \times (0,1],$$

$$u(0,t) = u(1,t) = u(x,0) = 0,$$

with

$$a(x,t) = \begin{cases} -(1+\exp(-xt)), & 0 \le x \le 0.5, t \in (0,1], \\ 2+x+t, & 0.5 < x \le 1, t \in (0,1], \end{cases}$$

$$f(x,t) = \begin{cases} (\exp(t^2)-1)(1+xt), & 0 \le x \le 0.5, t \in (0,1], \\ -(2+x)t^2, & 0.5 < x \le 1, t \in (0,1], \end{cases}$$

and $b(x,t) = 2 + xt$.

6 Discussion

Table 1: Maximum point-wise error $E^{N,M}$ and approximate orders of convergence $R^{N,M}$ for Example 1 when $\epsilon = 2^{-6}$.

μ	Number of mesh points N					
	32	64	128	256	512	1024
2^{-8}	4.17e-03	1.41e-03	6.13e-04	2.94e-04	1.45e-04	6.99e-05
Order	1.5623	1.2055	1.0627	1.0181	1.0526	
2^{-12}	3.24e-03	8.65e-04	2.26e-04	5.92e-05	1.58e-05	3.98e-06
Order	1.9038	1.9330	1.9357	1.9099	1.9891	
2^{-16}	3.22e-03	8.54e-04	2.21e-04	5.62e-05	1.42e-05	3.55e-06
Order	1.9902	1.9972	1.9991	1.9995	1.9991	
2^{-20}	3.21e-03	8.53e-04	2.20e-04	5.60e-05	1.41e-05	3.53e-06
Order	1.9132	1.9532	1.9753	1.9867	1.9979	
2^{-24}	3.21e-03	8.53e-04	2.20e-04	5.60e-05	1.41e-05	3.53e-06
Order	1.9132	1.9532	1.9761	1.9879	1.9979	
$\vdots$	$\vdots$	$\vdots$	$\vdots$	$\vdots$	$\vdots$	$\vdots$
2^{-60}	3.21e-03	8.53e-04	2.20e-04	5.60e-05	1.41e-05	3.53e-06
Order	1.9132	1.9532	1.9761	1.9880	1.9979	

Table 1 tabulates the error and numerical order of convergence for the Example 1 for different values of μ when $\epsilon = 2^{-6}$. Table 2 presents the numerical results for different values of ϵ and $\mu = 2^{-6}$ for Example 1. In Table 2, we note that the order of convergence for different values of ϵ increased till $N = 256$ and slightly decreased for $N = 512$. The numerical order of convergence for $N = 512$ is still two. This decrease in convergence is due

Table 2: Maximum point-wise error $E^{N,M}$ and approximate orders of convergence $R^{N,M}$ for Example 1 when $\mu = 2^{-6}$.

ϵ	Number of mesh points N				
	64	128	256	512	1024
2^{-16}	2.32e-01	9.41e-02	2.52e-02	5.63e-03	1.67e-03
Order	1.3012	1.9025	2.1589	1.7513	
2^{-20}	2.31e-01	1.03e-01	2.43e-02	5.57e-03	1.46e-03
Order	1.1738	2.0757	2.0678	1.9272	
2^{-24}	2.31e-01	1.03e-01	2.41e-02	5.48e-03	1.35e-03
Order	1.1643	2.0955	2.1374	2.0222	
2^{-28}	2.31e-01	1.03e-01	2.41e-02	5.47e-03	1.34e-03
Order	1.1638	2.0967	2.1415	2.0329	
2^{-32}	2.31e-01	1.03e-01	2.41e-02	5.46e-03	1.33e-03
Order	1.1637	2.0969	2.1424	2.0330	
2^{-36}	2.31e-01	1.03e-01	2.41e-02	5.46e-03	1.33e-3
Order	1.1637	2.0969	2.1424	2.0331	
2^{-40}	2.31e-01	1.03e-01	2.41e-02	5.47e-03	1.34e-03
Order	1.1637	2.0969	2.1424	2.0331	

Table 3: Maximum point-wise error $E_\epsilon^{N,M}$ and approximate orders of convergence $R_\epsilon^{N,M}$ for Example 1.

ϵ	Number of mesh points N				
	64	128	256	512	1024
10^{-2}	4.70e-03	2.25e-03	1.13e-03	5.69e-04	2.69e-04
Order	1.0632	0.9951	0.9871	1.0799	
10^{-4}	1.70e-01	6.05e-02	1.55e-02	3.88e-03	1.10e-03
Order	1.4912	1.9646	1.9982	1.8212	
10^{-6}	2.19e-01	9.18e-02	2.38e-02	5.79e-03	1.59e-03
Order	1.3947	2.0482	2.0955	2.0558	
10^{-8}	9.66e-02	4.22e-02	9.92e-03	2.37e-03	5.79e-04
Order	1.1963	2.0881	2.0654	2.0323	
10^{-10}	1.19e-01	4.22e-02	9.92e-03	2.37e-03	6.04e-04
Order	1.4918	2.0883	2.0667	2.0106	
10^{-12}	2.39e-01	8.09e-02	1.95e-02	4.58e-03	1.10e-03
Order	1.5658	2.0486	2.0938	2.0581	
10^{-14}	2.39e-01	8.09e-02	1.96e-02	4.58e-03	1.10e-03
Order	1.5658	2.0486	2.0938	2.0581	

Table 4: Maximum point-wise error $E^{N,M}$ and approximate orders of convergence $R^{N,M}$ for Example 2 when $\epsilon = 2^{-6}$.

μ	Number of mesh points N				
	64	128	256	512	1024
2^{-10}	4.67e-03	1.55e-03	6.01e-04	2.54e-04	1.20e-04
Order	1.5912	1.3668	1.2425	1.0818	
2^{-14}	4.00e-03	1.03e-03	2.62e-04	6.61e-05	1.66e-05
Order	1.9521	1.9751	1.9868	1.9939	
2^{-18}	4.00e-03	1.03e-03	2.63e-04	6.63e-05	1.66e-05
Order	1.9515	1.9750	1.9865	1.9938	
2^{-22}	4.00e-03	1.03e-03	2.63e-04	6.63e-05	1.67e-05
Order	1.9515	1.9750	1.9865	1.9938	
2^{-28}	4.00e-03	1.03e-03	2.63e-04	6.63e-05	1.67e-05
Order	1.9515	1.9750	1.9865	1.9938	
2^{-32}	4.00e-03	1.03e-03	2.63e-04	6.63e-05	1.67e-05
Order	1.9515	1.9750	1.9865	1.9938	
$\vdots$	$\vdots$	$\vdots$	$\vdots$	$\vdots$	$\vdots$
2^{-60}	4.00e-03	1.03e-03	2.63e-04	6.63e-05	1.67e-05
Order	1.9515	1.9750	1.9865	1.9938	

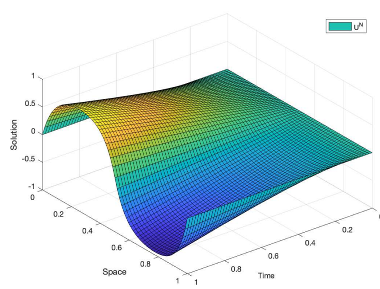

Figure 2: Numerical solution for $\epsilon = 2^{-6}, \mu = 2^{-32}$ when $N = 64$ for Example 1.

to the fact that in boundary layer region upwind scheme is replaced by the midpoint upwind scheme. The midpoint upwind scheme is not performing as well as the upwind scheme.

Figures 2 and 3 represent the surface plot of the numerical solution and error graph of Example 1, respectively, for $\mu = 2^{-32}$, $\epsilon = 2^{-6}$ and $N = 64$. We note that the maximum error is at the point of discontinuity. Figures 4 and

Table 5: Maximum point-wise error $E^{N,M}$ and approximate orders of convergence $R^{N,M}$ for Example 2 when $\mu = 2^{-6}$.

ϵ	Number of mesh points N				
	64	128	256	512	1024
2^{-18}	3.31e-01	1.51e-01	3.72e-02	9.95e-03	2.66e-03
Order	1.1321	2.0226	1.9015	1.9011	
2^{-22}	3.55e-01	1.55e-01	3.63e-02	9.75e-03	2.55e-03
Order	1.1982	2.0914	1.8940	1.9330	
2^{-26}	3.55e-01	1.55e-01	3.63e-02	9.75e-03	2.55e-03
Order	1.1982	2.0914	1.8940	1.9330	
2^{-30}	3.55e-01	1.55e-01	3.63e-02	9.75e-03	2.55e-03
Order	1.1982	2.0914	1.8940	1.9330	
2^{-34}	3.55e-01	1.55e-01	3.63e-02	9.75e-03	2.55e-03
Order	1.1982	2.0914	1.8940	1.9330	
2^{-38}	3.55e-01	1.55e-01	3.63e-02	9.75e-03	2.55e-03
Order	1.1982	2.0914	1.8940	1.9330	
2^{-42}	3.55e-01	1.55e-01	3.63e-02	9.75e-03	2.55e-03
Order	1.1982	2.0914	1.8940	1.9330	

Table 6: Maximum point-wise error $E^{N,M}$ and approximate orders of convergence $R^{N,M}$ for Example 3 when $\epsilon = 2^{-8}$.

μ	Number of mesh points N					
	32	64	128	256	512	1024
2^{-14}	7.74e-03	2.08e-03	5.31e-04	1.34e-04	4.79e-05	2.19e-05
Order	1.8947	1.9704	1.9834	1.4871	1.1292	
2^{-16}	7.83e-03	2.14e-03	5.62e-04	1.34e-04	3.36e-05	8.49e-06
Order	1.8692	1.9572	1.9654	1.9974	1.9858	
2^{-20}	7.86e-03	2.17e-03	5.69e-04	1.45e-04	3.85e-05	9.72e-06
Order	1.9108	1.9481	1.9657	1.9672	1.9868	
2^{-24}	7.86e-03	2.17e-03	5.69e-04	1.45e-04	3.85e-05	9.72e-06
Order	1.9902	1.9972	1.9991	1.9995	1.9872	
2^{-28}	7.86e-03	2.17e-03	5.69e-04	1.46e-04	3.73e-05	9.43e-06
Order	1.8592	1.9299	1.9605	1.9694	1.9845	
$\vdots$	$\vdots$	$\vdots$	$\vdots$	$\vdots$	$\vdots$	$\vdots$
2^{-60}	7.86e-03	2.1e-03	5.69e-04	1.46e-04	3.73e-05	9.43e-06
Order	1.8592	1.9299	1.9605	1.9694	1.9845	

Table 7: Maximum point-wise error E^N and approximate orders of convergence R^N for Example 3 when $\mu = 2^{-6}$.

ϵ	Number of mesh points N				
	64	128	256	512	1024
2^{-18}	2.28e-02	9.24e-03	2.87e-03	7.47e-04	1.97e-04
Order	1.3030	1.8330	1.9301	1.9221	
2^{-22}	2.27e-02	9.25e-03	2.54e-03	6.61e-04	1.73e-04
Order	1.2951	1.8634	1.9434	1.9339	
2^{-26}	2.27e-02	9.25e-03	2.54e-03	6.61e-04	1.73e-04
Order	1.2951	1.8634	1.9434	1.9339	
2^{-30}	2.97e-02	9.26e-03	2.54e-03	6.61e-04	1.73e-04
Order	1.2951	1.8634	1.9434	1.9339	
2^{-34}	2.97e-02	9.2561e-03	2.54e-03	6.61e-04	1.73e-04
Order	1.2951	1.8634	1.9434	1.9339	
2^{-38}	2.97e-02	9.26e-03	2.54e-03	6.61e-04	1.73e-04
Order	1.2951	1.8634	1.9434	1.9339	
2^{-42}	2.97e-02	9.26e-03	2.54e-03	6.61e-04	1.73e-04
Order	1.2951	1.8634	1.9434	1.9339	

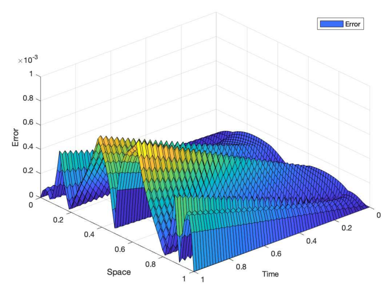

Figure 3: Error for $\epsilon = 2^{-6}, \mu = 2^{-32}$ when $N = 64$ for Example 1.

5 show the numerical solution and error graph for Example 1, respectively, when $\epsilon = 2^{-30}$, $\mu = 2^{-6}$, and $N = 128$. Here too the maximum error occurs at the point of discontinuity.

In Table 3, we present the maximum point-wise error and order of convergence for $\mu \in S = \{10^{-j}, j = 2, 4, 6.\}$ and for different ϵ. Tables 4 and 5 tabulate the value for different ϵ and μ for Example 2. In Figures 6 and 7, the numerical solution and error graph for Example 2, respectively, when

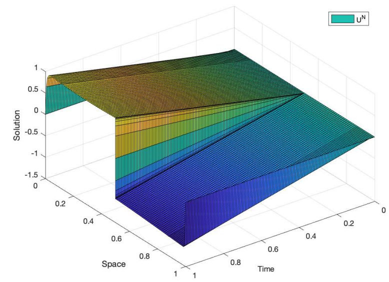

Figure 4: Numerical solution for $\epsilon = 2^{-30}, \mu = 2^{-6}$ when $N = 128$ for Example 1.

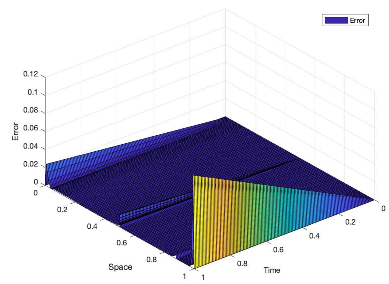

Figure 5: Error for $\epsilon = 2^{-30}, \mu = 2^{-6}$ when $N = 128$ for Example 1.

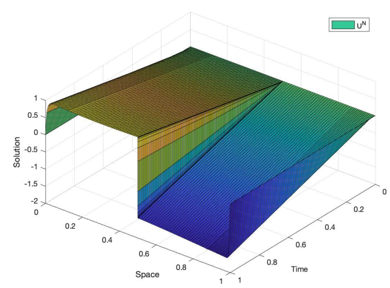

Figure 6: Numerical solution for $\epsilon = 2^{-22}, \mu = 2^{-6}$ when $N = 128$ for Example 2.

$\epsilon = 2^{-22}$, $\mu = 2^{-6}$, and $N = 128$ are presented. Here, the maximum error occurs at the boundaries near $x = 1$.

Similarly, Table 6 tabulates the error and numerical order of convergence for Example 3 for different values of μ when $\epsilon = 2^{-8}$. Table 7 tabulates the

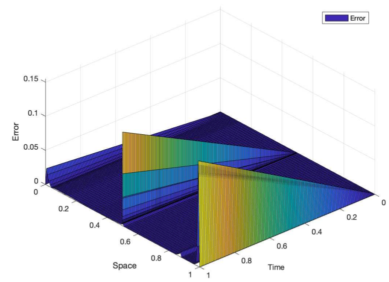

Figure 7: Error for $\epsilon = 2^{-22}, \mu = 2^{-6}$ when $N = 128$ for Example 2.

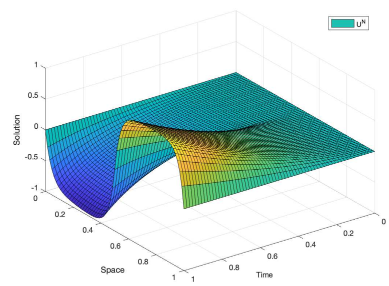

Figure 8: Numerical solution for $\epsilon = 2^{-8}, \mu = 2^{-36}$ when $N = 64$ for Example 3.

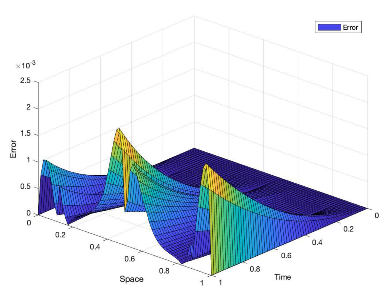

Figure 9: Error for $\epsilon = 2^{-8}, \mu = 2^{-36}$ when $N = 64$ for Example 3.

error and numerical order of convergence for Example 3 for different values of ϵ when $\mu = 2^{-6}$.

Figures 8 and 9 represent the surface plot of the numerical solution and error graph of Example 3, respectively, for $\epsilon = 2^{-8}$, $\mu = 2^{-36}$, and $N = 64$.

We note that the maximum error is at the point of discontinuity. Here, we also noted the same pattern in Tables 3, 5, and 7, as noted in Table 2, that is, the order of convergence is increased and then decreased for higher values of N.

7 Conclusions

In this article, we studied a singularly perturbed two-parameter parabolic problem characterized by a discontinuous convection coefficient and source term. The solution reveals boundary layers near the domain boundaries and internal layers at the point of discontinuity, induced by the discontinuities in the convection coefficient and source term. For the temporal discretization, we utilized the Crank–Nicolson method on a uniform mesh, achieving second-order accuracy in time. In the spatial direction, we implemented a hybrid difference scheme, which integrates the midpoint method, central difference method and upwind difference method on a suitably defined Shishkin mesh with a five-point formula at the discontinuity point, ensuring almost second-order accuracy in space. The theoretical analysis was corroborated by numerical results, demonstrating the efficacy and accuracy of the proposed approach.

Acknowledgements

Authors are grateful to the anonymous referees and the editor for their constructive comments.

References

[1] Bullo, T.A., Duressa, G.F. and Degla, G.A. *Higher order fitted operator finite difference method for two-parameter parabolic convection-diffusion problems*, Int. J. Eng. Technol. Manag. Appl. Sci. 11(4) (2019), 455–467.

[2] Cen, Z. *A hybrid difference scheme for a singularly perturbed convection-*

diffusion problem with discontinuous convection coefficient, Appl. Math. Comput. 169(1) (2005), 689–699.

[3] Chandru, M., Das, P. and Ramos, H. *Numerical treatment of two-parameter singularly perturbed parabolic convection diffusion problems with non-smooth data*, Math. Methods Appl. Sci. 41(14) (2018), 5359–5387.

[4] Chandru, M., Prabha, T., Das, P. and Shanthi, V. *A Numerical Method for Solving Boundary and Interior Layers Dominated Parabolic Problems with Discontinuous Convection Coefficient and Source Terms,* Differ. Equ. Dyn. Syst. 27 (2019), 91–112.

[5] Crank, J. and Nicolson, P. *A practical method for numerical evaluation of solutions of partial differential equations of the heat-conduction type*, Adv. Comput. Math. 7 (1996), 207–226.

[6] Das, P. *A higher order difference method for singularly perturbed parabolic partial differential equations*, J. Differ. Equ. Appl. 24(3)(2018), 452–477.

[7] Das, P. and Mehrmann, V. *Numerical solution of singularly perturbed convection-diffusion-reaction problems with two small parameters*, BIT Numer. Math. 56(1) (2016), 51–76.

[8] Farrell, P.A., Hegarty, A.F., Miller, J.J.H., O'Riordan, E. and Shishkin, G.I. *Robust Computational Techniques for Boundary Layers*, vol. 1. Chapman & Hall/CRC,New York, 2000.

[9] Gracia, G.L. and O'Riordan, E. *Numerical approximation of solution derivatives in the case of singularly perturbed time dependent reaction–diffusion problems*, J. Comput. Appl. Math. 273 (2015), 13–24.

[10] Gupta, V., Kadalbajoo, M.K. and Dubey, R.K. *A parameter-uniform higher order inite difference scheme for singularly perturbed time-dependent parabolic problem with two small parameters*, Int. J. Comput. Math. 96(3) (2018), 1–29.

[11] Kadalbajoo, M.K. and Yadaw, A.S. *Parameter-uniform finite element method for two-parameter singularly perturbed parabolic reaction-diffusion problems*, Int. J. Comput. Methods 9(4) (2012), 1250047.

[12] Kumar, D. and Kumari, P. *Uniformly convergent scheme for two-parameter singularly perturbed problems with non-smooth data*, Numer. Methods Partial Differ.Equ. 37(1) (2021), 796–817.

[13] Markowich, P.A. *A finite difference method for the basic stationary semiconductor device equations*. numerical boundary value ODEs (Vancouver, B.C.,1984), Progr. Sci. Comput., Vol. 5, Birkhäuser Boston, Boston, MA, (1985), 285–301.

[14] Mekonnen, T.B. and Duressa, G.F. *Computational method for singularly perturbed two-parameter parabolic convection-diffusion problems*, IMA J. Numer. Anal. 7(1) (2020), 1829277.

[15] Mukherjee, K. and Natesan, S. *ϵ-uniform error estimate of hybrid numerical scheme for singularly perturbed parabolic problems with interior layers*, Numer. Algorithms, 58 (2011), 103–141.

[16] Munyakazi, J.B. *A robust finite difference method for two-parameter parabolic convection-diffusion problems*, Appl. Math. Inf. Sci. 9(6)(2015), 2877–2883.

[17] O'Malley, R.E. *Introduction to Singular Perturbations*, Academic Press, New York, London, 1974.

[18] O'Riordan, E., Pickett, M.L. and Shishkin, G.I. *Singularly perturbed problems modeling reaction-convection-diffusion processes*, Comput. Methods Appl. Math. 3(3) (2003), 424–442.

[19] O'Riordan, E., Shishkin, G.I. and Picket, M.L. *Parameter-uniform finite difference schemes for singularly perturbed parabolic diffusion-convection-reaction problems*, Math. Comput. 75(255) (2006), 1135–1154.

[20] Schlichting, H. *Boundary Layer Theory*, seventh ed., McGraw-Hill, New York, 1979.

[21] Singh, S. and Kumar, D. *Parameter uniform numerical method for a system of singularly perturbed parabolic convection–diffusion equations,* Math. Comput. Simul. 212 (2023), 360–381.

[22] Singh, S., Choudhary, R. and Kumar, D. *An efficient numerical technique for two-parameter singularly perturbed problems having discontinuity in convection coefficient and source term*, Comput. Appl. Math. 42(62) (2023), 42–62.

[23] Stynes, M. and Roos, H.G. *The midpoint upwind scheme*, Appl. Numer. Math. 23(3) (1997), 361–374.

[24] Zahra, W.K., El-Azab, M.S. and El Mhlawy, A.M. *Spline difference scheme for two-parameter singularly perturbed partial differential equations*, Int. J. Appl. Math. 32(1-2) (2014), 185–201.